School of Molecular and Life Sciences (MLS)

Use of UV/Chlorine as Advanced Oxidation Processes

Amin Delfi

This thesis is presented for the Degree of
Master of Philosophy (Civil Engineering)
of
Curtin University

January 2021

Declaration

To the best of my knowledge and belief, this thesis contains no material previously published by any other person except where due acknowledgment has been made.

This thesis contains no material which has been accepted for the award of any other degree or diploma in any university.

Amin Delfi

Date: 01/01/2020

Abstract

The combination of ultraviolet (UV) irradiation and chlorination is regarded as a promising advanced oxidation process (AOP) to remove/reduce undesirable organic pollutants. However, a major drawback is the occurrence of disinfection by-products (DBPs) since predicting their formation is challenging. Therefore, the main focus of this study was to undertake experiments with water samples exhibiting different reactivities collected from two different sources; Mundaring Water Treatment Plant (MWTP) and Ceramic Membrance Pilot Plants (CMPP) to better understand the extent of DBPs formation during UV/chlorine treatment. The analysis of the water samples after oxidative treatment shows that the concentration of dissolved organic carbon (DOC) decreased by 9% during dark chlorination and UV/chlorine oxidation without a noticeable difference between the two treatment. The specific ultraviolet absorbance ($SUVA_{254nm}$) value significantly decreased during UV/chlorine oxidation compared to the dark chlorination with an average of 50.0% and 20.1%, respectively. Chlorine concentration was greatly reduced during UV/chlorine oxidation compared to dark chlorination for all samples. Chlorate formation was gradually increasing after UV/chlorine oxidation in all MWTP samples except in pre-Biological Activated Carbon (BAC) water sample after 24 h. No clear trend could be extrapolated based on the formation of adsorbable organic halides (AOX), trihalomethanes (THMs) and haloacetonitriles (HANs) after the experiments. However, total haloacetic acid (THAAs), total haloketons (THKs) and total haloacetaldehydes (THALs) formation increased significantly during UV/chlorine oxidation compared to dark chlorination. This clearly showed that the impact of UV is detrimental to the mitigation of HAAs, HKs and HALs, with 90% more THAAs and with ~ 2 times more THKs after 2000 mJ/cm^2 of UV compared to dark chlorination. Depending on the UV dose and the water characteristic, the UV/chlorine treatment could be beneficial in mitigation DBPs such as THMs, HANs and AOX. The applied chlorine concentration and UV dose should be carefully adjusted based on the goal that needs to be achieved, i.e. keeping the DBPs below the guideline values or reducing the formation of AOX for example.

Acknowledgment

I want to thank my supervisor, Dr. Sebastien Allard for his guidance, support, and technical advice during my project. I want to thank the Graduate Research School (GRS) and Curtin University for the financial support and for allowing me to work on this project.

I also want to thank the School of Molecular Life science (MLS) and Curtin Water Quality Research Group (CWQRG) for their support and for allowing me to work on my project in the CWQRG laboratory.

I am thankful to Dr. Yolanta Gruchlik, Peter Hopper, Peter Chapman, and all of the CWQRG research students for their support and help in carrying out this project.

I also want to thank my entire family and Dr. Indi Pattni for their endless support and encouragement in completing my project and thesis.

Table of Contents

List of Figures

List of Tables

List of Abbreviations

AOPs	Advanced oxidation processes
AOX	Absorbable organic halides
BAA	Bromoacetic acid
BAC	Biological active carbon
BAN	Bromoacetonitrile
BCAA	Bromochloroacetic acid
BCAL	Bromochloroacetaldehyde
BCAN	Bromochloroacetonitrile
BDCAA	Bromodichloroacetic acid
BDCM	Bromodichloromethane
Br^-	Bromide ion
Br-DBPs	Brominated disinfection by-products
BrO_3^-	Bromate ion
CAN	Chloroacetonitrile
CDBAA	Chlorodibromoacetic acid
CDBM	Chlorodibromomethane
CH	Chloral hydrate
Cl^-	Chloride ion
$Cl^\bullet$	Chlorine radical
$Cl_2^{\bullet-}$	Dichlorine radical anion
Cl_2	Chlorine molecule
Cl-DBPs	Chlorinated disinfection by-products
$ClO^\bullet$	Chlorine monoxide radical

199	ClO_2	Chlorine dioxide
200	ClO_2^-	Chlorite ion
201	ClO_3^-	Chlorate ion
202	ClO_4^-	Perchlorate ion
203	CMPP	Ceramic membrane pilot plants
204	CP	Chloropicrin
205	DAFF	Dissolved air flotation filtration
206	DBAA	Dibromoaceic acid
207	DBAL	Dibromoacetaldehyde
208	DBAN	Dibromoacetonitrile
209	DBCM	Dibromochloromethane
210	DBPs	Disinfection by-products
211	DCAA	Dichloroacetic acid
212	DCAL	Dichloroacetaldehyde
213	DCAN	Dichloroacetonitrile
214	DCBM	Dichlorobromomethane
215	DCP	1,1-Dichloropropanone
216	DOC	Dissolved organic carbon
217	EI	Electron ionisation
218	GC	Gas chromatography
219	GC-MS	Gas chromatography-mass spectrometry
220	HAAs	Haloacetic acids
221	HALs	Haloacetaldehydes
222	HANs	Haloacetonitriles

223	HKs	Haloketones
224	HNO_3	Nitric acid
225	H_2O_2	Hydrogen peroxide
226	HOBr	Hypobromous acid
227	HOCl	Hypochlorous acid
228	IC	Ion chromatograph
229	LLE	Liquid-liquid extraction
230	LP	Low pressure
231	MBAA	Monobromoacetic acid
232	MCAA	Monochloroacetic acid
233	MeOH	Methanol
234	$MgSO_4$	Magnesium sulphate
235	MP	Medium pressure
236	MSD	Mass selective detector
237	MTBE	Methyl tert-butyl ether
238	MWTP	Mundaring Water Treatment Plant
239	$NaHCO_3$	Sodium hydrogen carbonate
240	Na_2SO_4	Sodium sulphate
241	NOM	Natural organic matter
242	OCl^-	Hypochlorite ion
243	•OH	Hydroxyl radical
244	SIM	Selective ion monitoring
245	SPME	Solid-phase microextraction
246	SUVA	Specific ultraviolet absorbance

247	TBAA	Tribromoacetic acid
248	TBAL	Tribromoacetaldehyde
249	TBM	Tribromomethane
250	TCAA	Trichloroacetic acid
251	TCAN	Trichloroacetonitrile
252	TeCP	Tetrachloropropanone
253	TCM	Trichloromethane
254	TCP	1,1,1-Tichloropropanone
255	THAAs	Total haloacetic acids
256	THALs	Total haloacetaldehydes
257	THANs	Total haloacetonitriles
258	THKs	Total haloketones
259	THMs	Trihalomethanes
260	TTHMs	Total trihalomethanes
261	TOX	Total organic halides
262	UV	Ultraviolet
263	WWTPs	Wastewater treatment plants

Chapter 1: Introduction

1.1 Background

In recent years numerous micropollutants have been identified in various drinking water sources. Since some micropollutants are not efficiently removed by conventional municipal wastewater treatment plants (WWTPs), the quality of drinking water sources can deteriorate. To cope with this issue advanced oxidation processes (AOPs) have gained attention and ultraviolet (UV) based AOPs have been increasingly implemented to degrade organic micropollutants in the last decade.

Common chemical oxidants widely used for drinking water and wastewater treatment, such as chlorine, chloramine, and ozone are not efficient in degrading certain classes of micropollutants. Ultraviolet radiation (UV) has been increasingly used as a final disinfection method for water and wastewater due to its high germicidal effectiveness toward chlorine-resistant microorganisms and its low by-product formation. AOPs have been developed to specifically treat recalcitrant pollutants by using hydroxyl radicals ($^{\bullet}OH$). $^{\bullet}OH$ are non-selective and oxidise a wider spectrum of organic compounds than conventional oxidants (e.g., HOCl, ClO_2, and O_3). The most widely applied UV-based AOP is UV/H_2O_2 since H_2O_2 can be photolyzed into two $^{\bullet}OH$. However, the application of UV/chlorine has gained attention for several reasons. The relatively higher UV absorption of chlorine species than H_2O_2, induces a higher yield of $^{\bullet}OH$ generation. Therefore, it has been shown that UV/chlorine is more cost-effective than UV/H_2O_2 for the removal of pharmaceuticals and personal care products (Sichel, Garcia, & Andre, 2011). The UV/chlorine process not only produces $^{\bullet}OH$ but also generates reactive chlorine species i.e. $Cl^{\bullet}$, $Cl_2^{\bullet-}$ and $ClO^{\bullet}$. These species might also participate in the degradation of some micropollutants. Finally, each process is already commonly used separately in different parts of the treatment train, and implementing UV/HOCl does not require extensive additional infrastructure. The UV/chlorine process also has the advantage that it provides a disinfectant residual which is mandatory in many countries. It is a multi-barrier system since it combines, an AOP and a disinfectant residual for the distribution system.

One of the greatest achievements over the last century regarding public health has been the use of chemical disinfectants to produce potable drinking water. Chlorine is the most cost-effective approach in achieving both primary and secondary disinfection in

the distribution system worldwide. However, one of the unintended consequences of using disinfectants in the drinking water system is the formation of halogenated DBPs. They are resulting from the reaction of NOM or anthropogenic organic compounds with chlorine (bromine if bromide is present).

Although the use of UV/chlorine system seems attractive since it degrades recalcitrant micropollutants, its effect on the formation or behaviour of regulated/unregulated chlorinated DBPs is still unclear and is the impetus of this study.

1.2 Objectives

The broad aims of this research was to understand the formation of different types of DBPs during UV/chlorine oxidation in water treatment systems based on a review of published work along with laboratory studies as described below. The study outcomes will lead to improved knowledge on the impact of UV/chlorine treatment on the DBPs formation in real drinking water treatment plant of Western Australia.

In order to understand the formation of DBPs during UV/chlorine treatment, water samples were collected from two water sources MWTP and CMPP. To study the effect of different UV fluences, two UV doses of 1000 and 2000 mJ/cm^2 were used before chlorine was applied to the different water samples. DBPs formation, including HAAs, THMs, HANs, HKs, HALs and AOX under different experimental conditions was investigated. The formation of DBPs from UV/chlorine was compared with dark chlorination performed under the same experimental conditions such as chlorine dose, reaction time, temperature and pH.

The main focus of the study was to compare the formation of HAAs, THMs, HANs, HKs, HALs and AOX during UV/chlorination with chlorination alone since inconsistent results were obtained in previous studies.

Chapter 2: Literature review

2.1 UV/chlorine process

As mentioned in the previous paragraph, AOP mostly relies on $^{\bullet}OH$ reactions. However, during the UV/chlorine process chlorinated reactive species are also formed such as $Cl^{\bullet}$, $Cl_2^{\bullet-}$ and $ClO^{\bullet}$. It is important to notice that this is different from the UV/H_2O_2 process which is solely producing $^{\bullet}OH$ since in the UV/chlorine process the main scavenger of $^{\bullet}OH$ might be the chlorine species themselves. In a recent study, it was demonstrated that the steady-state $^{\bullet}OH$ concentration in UV/HOCl was higher than that in UV/OCl^- by a factor of 23.3. This was attributed to the different $^{\bullet}OH$ consumption rates by HOCl versus OCl^- (W. Lee et al., 2020). This illustrates that the pH will play an important role in both the steady-state concentration of $^{\bullet}OH$ and the formation of halogenated radical species. Another important parameter that needs to be taken into consideration during the UV/chlorine process is the formation of oxyhalides species that are not formed during conventional chlorination. These oxyhalides are formed following a complex suite of reactions involving chlorinated radicals as depicted in W.Lee et.al (2020). Chlorite (ClO_2^-) and chlorate (ClO_3^-) are regulated with guidelines set at 0.7 mg L^{-1} by the world health organization (WHO) (the European Commission is considering setting an even lower value of 0.25 mg L^{-1}) (EUC, 1998; WHO, 2011). Bromate (BrO_3^-) which is a probable human carcinogen is regulated at 10 µg L^{-1} in drinking water standards in most countries (20 µg L^{-1} in Australia) (NWQMS, 2011; USEPA, 2006; WHO, 2011). This has an important implication since it was reported in Lee et.al (2020) that the level of ClO_3^- and BrO_3^- formed during the UV/chlorine process can exceed the guideline. In such cases even though the UV/chlorine process allows to degrade recalcitrant pollutants, it won't be a suitable option for drinking water production. This also highlight the fact that these inorganic DBPs needs to be carefully controlled and not only the organic DBPs. Besides the formation of organic DBPs from conventional dark chlorination, the chlorinated reactive species might also participate to the formation of organic DBPs. It has been shown in numerous studies that $Cl^{\bullet}$, $Cl_2^{\bullet-}$ and $ClO^{\bullet}$ are reacting with organic compounds and therefore can participate to the pool of halogenated DBPs formation (Bulman & Remucal, 2020; D. Wang, Bolton, Andrews, & Hofmann, 2015; J. Wang & Wang, 2020; Xiang, Fang, & Shang, 2016).

2.2 Micropollutants degradation

The UV/Chlorine process is used as an AOP, i.e. for the degradation of micropollutant recalcitrant to regular oxidative processes. Therefore, numerous studies have investigated the degradation of micropollutants during UV/chlorine oxidation compared to the other treatments (Guo et al., 2017; Guo et al., 2018; Li, Jain, Ishida, Remucal, & Liu, 2017; Yeom et al., 2021). The structural properties of the micropollutants have a direct impact on their degradation by UV/chlorine oxidation due to reactive chlorine species such as $Cl^{\bullet}$, $Cl_2^{\bullet-}$ and $ClO^{\bullet}$ which react with electron-donating compounds (Lado Ribeiro, Moreira, Li Puma, & Silva, 2019; Yeom et al., 2021). According to Yeom et al. (2021), the roles of different radicals to micropollutant degradation are structure-dependent. In the degradation of micropollutants, hydroxyl radical has the leading role in the electron-withdrawing functional group but they are non specific (Yeom et al., 2021). Chlorine radical reacts quickly with aromatic compounds like phenols and benzoic acid (Guo et al., 2017; Lado Ribeiro et al., 2019). Different factors such as water matrix, UV dose, pH and chlorine dose influence the efficiency of micropollutant degradation during UV/chlorine oxidation. UV/chlorine treatment is typically more efficient for micropollutant degradation in acidic conditions and without scavengers like NOM and halide ions (Yeom et al., 2021). Even though, UV/Chlorine oxidation is used to degrade micropollutant, DBPs are still formed and it is important to understand which type and amount are produced compare to dark chlorination.

2.3 Formation of DBPs

2.3.1 Dark Chlorination

Free chlorine is utilized worldwide as a primary disinfectant in many water treatment plants to control waterborne diseases and inactive pathogens. However, during the chlorination process, DBPs are produced and need to be controlled. DBPs are mostly formed from the reaction of chlorine or bromine, since water ubiquitously contains bromide, with NOM (Glezer, Harris, Tal, Iosefzon, & Lev, 1999; Kristiana, Gallard, Joll, & Croué, 2009; Nieuwenhuijsen, Toledano, Eaton, Fawell, & Elliott, 2000; Richardson, 2003; Westerhoff, Chao, & Mash, 2004).

Bromide is rapidly oxidized by HOCl to hypobromous acid (HOBr) (Kumar & Margerum, 1987) and in many cases, the reactivity of HOBr in oxidation and halogenation reactions far outweighs the reactivity of HOCl (Amy, Chadik, King, & Cooper,

388 1984; Gallard, Pellizzari, Croué, & Legube, 2003; G. Hua, Reckhow, & Kim, 2006;
389 Y. Lee & Gunten, 2009). It was shown that the second-order rate constants for reac-
390 tions with phenolic compounds are on average 3000 times higher for HOBr compared
391 to HOCl (Heeb, Criquet, Zimmermann-Steffens, & von Gunten, 2014). Therefore, bro-
392 minated disinfection by-products (Br-DBPs) may be formed with higher rates and
393 yields than chlorinated disinfection by-products (Cl-DBPs).

394 The formation of Cl-DBPs has been extensively studied as well as their genotoxicity,
395 carcinogenicity, and mutagenicity (Matilainen & Sillanpää, 2010; Muellner et al.,
396 2007; Nieuwenhuijsen et al., 2000; Plewa, Muellner, et al., 2008; Plewa, Simmons,
397 Richardson, & Wagner, 2010; Plewa et al., 2004; M. J. Plewa et al., 2012; Plewa,
398 Wagner, Muellner, Hsu, & Richardson, 2008b, 2008c; Richardson, Plewa, Wagner,
399 Schoeny, & Demarini, 2007; Smith, Plewa, Lindell, Richardson, & Mitch, 2010;
400 USEPA, 1999; Y. Yang et al., 2014). The rapid formation of Br-DBPs is also of con-
401 cern since these compounds are more toxic than their chlorinated analog and generally
402 increased toxicity has been observed in chlorinated waters containing high concentra-
403 tions of bromide (P. Neale et al., 2012; Plewa, Muellner, et al., 2008; Plewa et al.,
404 2010; Plewa, Wagner, Muellner, Hsu, & Richardson, 2008a).

405 The formation of DBPs was discovered in 1974 when chloroform (TCM), the most
406 commonly regulated DBPs, was first detected in chlorinated drinking water (Johannes,
407 1976; USEPA, 1999). To date over seven hundred halogenated DBPs have been re-
408 ported, which represents only roughly 50% of the total organic halides (TOX) (Hansen
409 et al., 2012; Matilainen & Sillanpää, 2010; Richardson, 2003; USEPA, 1999, 2002).

410 The most common DBPs formed during chlorination are THMs and haloacetic acids
411 (HAAs) and are regulated in many countries (AWWA, 1999; Glezer et al., 1999;
412 Nieuwenhuijsen et al., 2000; Tchobanoglous, Burton, Stensel, Metcalf, & Eddy,
413 2003). Trichloromethane (TCM), bromodichloromethane (BDCM), chlorodibromo-
414 methane (CDBM), Tribromomethane (TBM) are trihalomethanes (THMs) (iodinated
415 DBPs are excluded). Haloacetic acids (HAAs) are the next important group and in-
416 clude 9 compounds namely chloroacetic acid (CAA), bromoacetic acid (BAA), di-
417 chloroacetic acid (DCAA), dibromoacetic acid (DBAA), bromochloroacetic acid
418 (BCAA), bromodichloroacetic acid (BDCAA), chlorodibromoacetic acid (CDBAA),
419 trichloroacetic acid (TCAA) and tribromoacetic acid (TBAA). Among these 9 HAAs,

DCAA, and TCAA are the most frequently reported during chlorination (AWWA, 1999; Gary et al., 1999; USEPA, 2002). However, during chlorination other classes of DBPs which are not always regulated can be formed such as haloacetonitriles (HANs), haloketons (HKs), and chloropicrin (CP) but usually at much lower concentration and might be more toxic than THMs and HAAs (Gary et al., 1999; Glezer et al., 1999; Muellner et al., 2007; Plewa, Wagner, et al., 2008b; USEPA, 1999; X. Yang, Shang, & Westerhoff, 2007).

2.3.2 Impact of UV on the generation of DBPs

UV does not directly impact the formation of halogenated DBPs. However, it does have an indirect impact since UV photolysis can modify the structure of NOM and therefore its reactivity with oxidant. For example, it has been shown that NOM containing high molecular weight compounds breaks down to lower molecular weight molecules in conjunction with the formation of carboxyl as well as carbonyl functional groups after exposition to UV (Corin, Backlund, & Kulovaara, 1996; Kulovaara, Corin, Backlund, & Tervo, 1996). Furthermore, UV can also affect the stability of halogenated DBPs if they are already present in the treated or source water.

It has been demonstrated that common DBPs (THMs, HAAs, HANs, HKs, and CP), as well AOX, are going through a slow photodecomposition process when exposed to increasing UVexposures (Corin et al., 1996; Deng, Huang, & Wang, 2014; Hansen, Zortea, Piketty, Vega, & Andersen, 2013; Höfl;, Sigl;, Specht;, Wurdack;, & Wabner, 1997; Jing Li & Blatchley, 2007; Kulovaara et al., 1996; Weng, Li, & Blatchley, 2012). Both brominated and chlorinated DBPs are affected by UV irradiation. Brominated compounds are typically more vulnerable to UV light compared to chlorinated compounds (Hansen et al., 2013; Jo, 2008).

The impact of UV on NOM reactivity with oxidant is more complex and strongly depends on the original NOM characteristics, the UV dose, the type of UV lamp, and the presence of inorganic compounds. The formation of DBPs from subsequent dark chlorination was shown to be dependent on the UV dose in some studies. It has to be noticed that for doses typically used for UV-disinfection (40 mJ/cm^2) a really low impact on DBP formation was observed. THMs, HAAs, and AOX formation were not affected by low UV exposure in several studies (W. Liu et al., 2002; Lyon, Dotson, Linden, & Weinberg, 2012; Malley Jr., Shaw, & Ropp, 1995; Marion, Weinberg, Dotson, &

452 Linden, 2010; Ramesh D et al., 2004; Reckhow, Linden, Kim, Shemer, & Makdissy,
453 2010). However, for highest UV doses, increased concentration of THMs, HAAs, and
454 AOX were observed after exposure to UV (low pressure (LP) or medium pressure
455 (MP)) pre-treatment with a fluence of 60 mJ/cm^2 (Wei Liu, Cheung, Yang, & Shang,
456 2006; Wei Liu, Zhang, Yang, Xu, & Liang, 2012). The choice of the lamp is also a
457 critical parameter. Lyon et al., (2012) reported that UV pre-treatment with MP with a
458 fluence of 1000 mJ/cm^2 increased TCM concentration by 30-40% while the HAAs
459 were not affected after 24 h of dark chlorination. Using the LP lamp with a similar
460 fluence of 1000 mJ/cm^2 did not impact the formation of THMs and HAAs. This is
461 consistent with a study from Dotson et al. (2010) to some extent. Dotson et al. (2010)
462 reported that using an MP lamp increased the concentration of THMs, significantly
463 compared to an LP lamp. However, contrasting results were obtained for HAAs with
464 a lower formation observed with the LP lamp and a higher concentration observed for
465 the MP lamp compared to dark chlorination. Lui et al., (2002) observed a different
466 effect of UV on DBPs formation compared to the other study. According to Lui et al.,
467 (2002) UV pre-treatment did not have a significant impact on the formation of THMs
468 and HAAs with a fluence of 5000 mJ/cm^2 in secondary chlorination. Similarly, Toor
469 and Mohseni (2007) observed no impact of UV pre-treatment with a fluence of 2500
470 mJ/cm^2 on THMs formation compared to dark chlorination. It was also reported that
471 the formation of CP was higher when an MP lamp compared to an LP lamp (Lyon et
472 al., 2012). The MP lamp indorses the formation of reactive nitrogen species. NOM can
473 react with these reactive nitrogen species to generate CP (Lyon et al., 2012; Reckhow
474 et al., 2010; Shah, Dotson, Linden, & Mitch, 2011).

475 ***2.3.3 UV/Chlorination***

476 In addition to the previously reported formation of DBPs by dark chlorination and
477 impact of UV on NOM reactivity, during UV/chlorine treatment, halogenated DBPs
478 might be formed by direct reaction of $Cl^{\bullet}$, $Cl_2^{\bullet-}$ or $ClO^{\bullet}$ with DOM. Furthermore, in-
479 organic DBPs, for instance, ClO_2^-, ClO_3^-, ClO_4^-, and BrO_3^-can also form and be the
480 main factor hindering the use of UV/chlorine (Buxton & Subhani, 1972a, 1972b,
481 1972c; Deng et al., 2014; Gunten & Hoigne, 1994; Kang, Anderson, & Andrew
482 Jackson, 2006; Pisarenko, Stanford, Snyder, Rivera, & Boal, 2013). It has been re-
483 cently shown that the formation of ClO_3^-, and BrO_3^- could potentially reach a level that
484 is above the guideline or recommended values (W. Lee et al., 2020). This makes the

UV/chlorine system one of the most complicated AOP with regards to DBPs formation.

There is no clear understanding with regards to $Cl^{\bullet}$, $Cl_2^{\bullet-}$ or $ClO^{\bullet}$ reaction with NOM. Some studies mentioned that $Cl^{\bullet}$has no significant role in the formation of DBPs (Nowell & Hoigné, 1992; Watts & Linden, 2007). On the other hand, numerous studies have been carried out on the reactivity of $Cl^{\bullet}$, $Cl_2^{\bullet-}$ or $ClO^{\bullet}$ with different types of organic compounds. For example, in a study done by Fang et al. (2014), $Cl^{\bullet}$reacts with benzoic acid, suggesting that chlorinated DBPs might be formed with NOM constituents of similar structure. It was recently demonstrated by high-resolution mass spectroscopy that $Cl^{\bullet}$ and $Cl_2^{\bullet-}$ are participating in the pool of halogenated DBPs formation (Bulman & Remucal, 2020; W. Lee et al., 2020).

Several studies have been comparing the formation of DBPs from UV/chlorine with dark chlorination (Ben, Sun, & Huang, 2016; Bulman & Remucal, 2020; Z. Hua et al., 2021; Wei Liu et al., 2006; Remucal & Manley, 2016; Shah et al., 2011; C. Wang, Moore, Bircher, Andrews, & Hofmann, 2019; D. Wang et al., 2015; Zhang, Li, Blatchley, Wang, & Ren, 2015). Pisarenko et al. (2013) observed that the HAAs formation was increased by 50% while no change in the formation of THMs was observed and the AOX formation was decreasing in UV/chlorination compared to dark chlorination. Plewa et al., (2012) and Wang et al., (2017) found an opposite trend with an increase in AOX concentration during UV/chlorination compared to dark chlorination. The formation of HANs was found to be higher in UV/chlorination compared to dark chlorination, according to Zhang et al., (2015), Weng et al. (2012), and Wang et al., (2015). Chloropropanone (CP) concentration was found to increase significantly in UV/chlorination compared to dark chlorination, according to several studies (Deng et al., 2014; W.-L. Wang et al., 2017; Yi Yang, Pignatello, Ma, & Mitch, 2016). Overall, various factors influence the generation of halogenated DBPs such as UV fluence, type of lamp, NOM characteristics, chlorine dose, and contact time during UV/chlorination. Therefore, even though UV/chlorine is regarded as a promising AOP to remove/reduce undesirable DBPs and organic pollutants, it is really difficult to predict the formation of DBPs. More works need to be carried out to better understand the mechanisms and the extend of DBPs formation under a different scenario.

Chapter 3: Materials and Methods

3.1 Water samples

Water samples were collected from two water sources, the Mundaring Water Treatment Plant (MWTP) and the effluent of a Ceramic Membrane Pilot Plants (CMPP), in 4-litre amber glass bottles. Water samples from MWTP were collected at four different locations: raw water, pre-dissolved air flotation filtration (DAFF), pre- biological active carbon (BAC), and post-BAC. Each step of the water treatment train has an impact on the raw water characteristics. Therefore, each sample exhibited different NOM characteristics due to specific treatment applied. This will allow to better understand the impact of the UV/Chlorine process on DBPs formation at different location in the water treatment train.

Figure 1. Mundaring Treatment Plant, pumping station, and integration work.

All bottles were filled with the water samples, leaving no headspace. All water samples were filtered with MicronSepNitrocelluloso 47 mm 0.45 µm membrane disks in the laboratory at Curtin University before the experiment.

3.2 Analytical Methods

3.2.1 Haloacetic Acids (HAAs)

Nine chlorinated and brominated HAAs were analysed. Monochloroacetic acid (MCAA), monobromoacetic acid (MBAA), bromodichloroaceticacid (BDCAA), DCAA, DBAA, BCAA, CDBAA, TCAA and TBAA. A stock solution of nine HAAs compounds was provided in methyl tert-butyl ether (MTBE) at 2 g/L. The surrogate standard and internal standard stock solutions (1 g/L) were prepared by spiking the desired volume of bromopropionic acid and 1, 2-dibromopropaneinto 10 mL acetone, respectively. These chemicals (surrogate and internal standards) were used for insuring a good qualitative and quantitative analysis (Carter, Allard, Croué, & Joll, 2019; Carter, Liew, West, Heitz, & Joll, 2019). Working solutions of high and low concentrations (100 mg/L and 10 mg/L) of HAAs were prepared by diluting the stock solution in acetone. Similarly, the surrogate standard working solution (50 mg/L) was prepared by diluting the stock solution in acetone, and the internal standard working solution (10 mg/L) was prepared by diluting of stock solution in MTBE. All calibration standards were prepared by spiking the right volume of working solutions into ultrapure water (50 mL). A sequence of standard solutions was prepared from 0 to 500 µg/L. The concentration of analytes in the unknown sample was expected to be in this range.

Liquid-liquid extraction (LLE) and derivatization method were used to extract HAAs. For the extraction process, a 60 mL glass vial was filled with 50 mL ultrapure water and 10 µL of working surrogate standard was spiked to the 50 mL water sample. The pH of the water was adjusted by adding 1 mL of concentrated sulphuric acid (H_2SO_4). Sodium sulphate (Na_2SO_4) (20 g), which was pre-baked at 400 °C was added to the sample. MTBE (3 mL) was spiked to the sample and agitated thoroughly for 4 min in a shaker. Then, the samples were left for 5 min to allow the separation of the organic and aqueous phases. After the phase separation, the organic layer (top layer) was collected and transferred to a 40 mL glass vial. 10% sulphuric acid was prepared in methanol (MeOH), and 2 mL of the solution was added to the vial (40 mL) for methylation. The samples were kept in a hot water bath (at 50 °C) for two hours. After two hours, the samples were allowed to cool down for a few minutes. Next, 2 mL of Na_2SO_4 solution (15 g of Na_2SO_4 dissolved in 100 mL of ultrapure water) was added to the sample. Then, the bottom layer was taken out with the help of a pipette and discarded. In the neutralisation step, 1 mL of saturated sodium hydrogen carbonate ($NaHCO_3$)

568 solution was added. The $NaHCO_3$ solution was prepared by dissolving $NaHCO_3$ in one
569 litre of ultrapure water until saturation and filtering the solution to remove any undis-
570 solved $NaHCO_3$. After adding the saturated $NaHCO_3$ solution to the sample, the or-
571 ganic layer was filtered through magnesium sulphate ($MgSO_4$) and directly placed into
572 a 1 mL gas chromatography (GC) vial. The sample was spiked with 10 µL of internal
573 standard and the GC vial capped. Then, the sample was analysed using GC-MS.

574 The HAAs were analysed on an Agilent 7890A gas chromatograph coupled with an
575 Agilent 5975C mass selective detector (MSD) running in electron ionisation (EI) mode
576 (70 eV) under the following conditions: MS Quad, 150 °C; MS source, 230 °C, and
577 MSD transfer, 250 °C. The injection was carried out in pulsed splitless mode under
578 the following conditions: syringe size, 10 µL; injection volume, 1 µL; purge time, 0.5
579 min and purge flow rate, 60 mL/min. GC separation was carried out on a DB -1701
580 (30 m x 250 µm x 1 µm) column under the following conditions: carrier gas, helium;
581 gas flow rate, 1 mL/min; initial temperature, 35 °C and hold time, 0 min. The oven
582 temperature conditions were as follows equilibration time: 3 min, temperature at 0
583 min, 35 °C; heated to 220 °C at 10 °C/min and held for 6 min. Where the final heating
584 occurred after elution of all target analytes with the purpose of conditioning the GC
585 column, the total instrumental runtime was 24.5 min. Selective ion monitoring (SIM)
586 was used for analyte identification and quantification using the mass-to-charge (m/z)
587 ratios provided in Table 1.

588 *Table 1. Mass to charge ratio (m/z) of different fragments of nine analytes (HAAs)*

Analytes	Formula	Characteristic m/z Ions	
		Quantification Ions	Target ions
Monochloroacetic Acid	MCAA	59	77, 108
Monobromoacetic Acid	MBAA	93	121, 152, 59
Dichloroacetic Acid	DCAA	59	83, 85
Trichloroacetic Acid	TCAA	59	117, 119, 141
Bromochloroacetic Acid	BCAA	59	129, 127, 131
Bromodichloroacetic Acid	BDCAA	163	161, 59, 141
Dibromoacetic Acid	DBAA	173	171, 59, 175
Chlorodibromoacetic Acid	CDBAA	207	59, 209, 205
Tribromoacetic Acid	TBAA	251	253, 59, 172

590 ***3.2.2 Trihalomethanes (THMs) and Haloacetonitriles (HANs)***

591 In this project, 4 THMs i.e. bromoform (TBM), dibromochloromethane (DBCM), di-
592 chlorobromomethane (DCBM), and chloroform (TCM) were quantified. Six HANs,
593 i.e., chloroacetonitrile (CAN), dichloroacetonitrile (DCAN), trichloroacetonitrile
594 (TCAN), bromoacetonitrile (BAN), bromochloroacetonitrile (BCAN) and dibromo-
595 acetonitrile (DBAN) were analysed. 1, 2-dibromopropane was used as an internal
596 standard, (Sebastien Allard, Charrois, Joll, & Heitz, 2012; Bond, Goslan, Parsons, &
597 Jefferson, 2012; Bond, Templeton, & Graham, 2012). A mixture of THMs compound
598 was prepared as a stock solution (2000 mg/L) into 10 mL MeOH. Similarly, HANs
599 stock solution (1000 mg/L) was prepared by mixing all the HAN compounds into 10
600 mL of MeOH. Working standard solutions of THMs (10 mg/L) and HANs (1 mg/L)
601 were prepared by spiking 50 and 10 µL of THMs and HANs stock solution into 10 mL
602 MeOH, respectively. 5.0 µL of 1, 2-dibromopropane was spiked in 10 mL of MeOH
603 to prepare the internal standard solution (1000 mg/L). A working internal standard
604 solution (5 mg/L) was prepared by adding 50 µL of the internal stock solution into 10
605 mL MeOH. A sequence of standard solutions was prepared with concentrations of an-
606 alytes ranging from 0 to 100 µg/L. The concentration of analytes in an unknown sam-
607 ple was expected to be in this range based on previous literature and experiments.

608 A solid-phase microextraction (SPME) method was used to extract the analytes from
609 the liquid phase. The SPME technique consisted of two stages: separation of the ana-
610 lytes from the aqueous to the gas phase and adsorption onto the SPME fiber (extraction
611 phase), and desorption of the enriched sample from the SPME fiber into the GC appa-
612 ratus (Fanali, 2013). The SPME method was used to extract concomitantly THMs and
613 HANs. The grey SPME fiber (DVB-CAR-PDMS) Supelco 57298-U was used for this
614 analysis. 20 mL amber GC vials were filled with 10 mL of sample. The water sample
615 was spiked with 10 µL of the internal standard working solution. 3.60 g of sodium
616 sulphate was added to the sample to increase the ionic strength and favor the extraction
617 of the analytes from the aqueous to the gas phase, which was then capped with a mag-
618 netic screw cap. Then, the samples were run on a GC-MS.

619

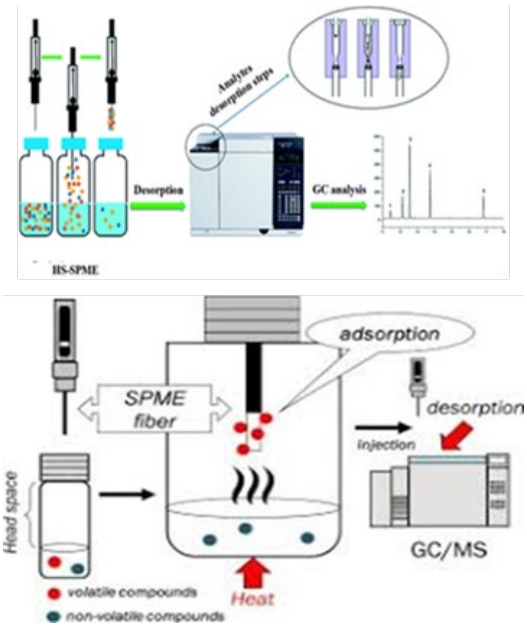

Figure 2. Schematic of Solid-phase micro-extraction (SPME) GC-MS

SPME analysis was carried out on an Agilent 6890N GC with an Agilent 5975 inert MSD. The injection was carried out in splitless mode to maximise the amount of analyte on the column, under the following condition: purge time; 1.0 min, purge flow rate; 104 mL/min, and carrier gas; helium. The SPME fiber was inserted in the headspace of the vial for 15 min at 50 ˚C. Then the fiber was inserted into the injector for 300 seconds at 220 ˚C. GC separation was performed on a ZB-5MS (30 m x 0.25 mm x 1 µm) column in constant flow mode under the following conditions: initial flow rate; 1.1 mL/min and max temperature, 325 °C. The oven conditions were as follow: initial temp, 40 °C; initial time, 5 min, and run time, 43.87 min. A fiber conditioning was run first before any set of injections.

Table 2. Mass to charge ratio (m/z) of different fragments of nine analytes (THMs and HANs)

Analytes	Formula	Characteristic m/z Ions	
		Quantification Ions	Target Ions
Bromoform	TBM	173	175
Dibromochloromethane	DBCM	129	127, 131
Dichlorobromomethane	DCBM	83	85,127, 129
Chloroform	TCM	83	85
Trichloroacetonitrile	TCAN	108	73, 82
Chloroacetonitrile	CAN	75	48, 50
Dichloroacetonitrile	DCAN	74	47, 76, 84
Bromoacetonitrile	BAN	119	79, 81
Bromochloroacetonitrile	BCAN	74	76, 93, 118, 120
Dibromoacetonitrile	DBAN	120	81, 91, 93, 197, 201

634 ***3.2.3 Haloketones (HKs) and Haloacetaldehydes (HALs)***

635 Four chlorinated HKs, chloropropanone (CP), 1,1-dichloropropanone (1,1-DCP), 1, 1,
636 1-trichloropropanone (1,1,1-TCP) and 1, 1, 3, 3-Tetrachloropropanone(1,1,3,3-TeCP)
637 were analysed. Six chlorinated and brominated HALs, dichloroacetaldehyde (DCAL),
638 dibromoacetaldehyde (DBAL), bromochloroacetaldehyde (BCAL), dibromochloroa-
639 cetaldehyde (DBCAL), Chloral hydrate (CH) and tribromoacetaldehyde (Bromal or
640 TBAL), were analysed. 1, 2-dibromopropane and 1, 1, 2, 2-tetrabromoethane were
641 used as the surrogate and internal standards, respectively. The surrogate was dissolved
642 in acetone (Carter, Allard, et al., 2019; María Serrano, Silva, & Gallego, 2014; Maria
643 Serrano, Silva, & Gallego, 2015). All stock solutions, for the analytes, the internal
644 standard, and the surrogate, were prepared with a final concentration (1 g/L) in acetone
645 by weighing or spiking the appropriate amount or volume of neat compounds. The
646 high working standard solutions (100 mg/L) were prepared by spiking 500 µL of HKs
647 and HALs stock solutions into 5 mL acetone. The low working standard solution (10
648 mg/L) was prepared by adding 50 µL of HKs and HALs stock solutions into 5 mL
649 acetone. The surrogate standard working solution (100 mg/L) was prepared by spiking
650 500 µL of the stock solution into 5 mL acetone. 50 µL of the stock solution (internal
651 standard) was added into 5 mL MTBE to prepare an internal standard working solution
652 (10 mg/L). A sequence of standard solutions was prepared from 0 to 100 µg/L.

653 A LLE method was used to extract HKs and HALs. A 60 mL LLE vial was filled with
654 50 mL of the sample. The sample pH was adjusted to pH 4 by adding concentrated
655 HCl. 10 µL of the surrogate standard working solution was added to the water sample.
656 20 µg/L is the concentration of the surrogate standard in the water sample. Next, 3 mL
657 of MTBE was added to the 50 mL water sample and capped. The water sample was
658 vigorously shaken by hand for 4 min. The sample was left a few minutes to rest after
659 shaking to allow for the aqueous and organic phases to separate. Then the top layer
660 (organic layer) was collected (1 mL) and dried by filtering through $MgSO_4$ into a GC
661 vial. Finally, 1 mL of the extract was spiked with 10 µL internal standard working
662 solution.

663 The HKs and HALs analysis was done on an Agilent 6890N GC coupled with an Ag-
664 ilent 5975 inert MSD (MSD). The injection was performed in the splitless mode under
665 the following conditions: purge time, 1.50 min; purge flow rate, 100 mL/min, and the
666 carrier gas was helium. GC separation was carried out on a ZB-5MS (30 m x 0.25 mm

x 1 µm) column in constant flow mode under the following conditions i.e. flow rate: 1.0 mL/min and max temperature, 325 °C. The oven conditions were as follows: Initial temp, 40 °C holds for 5 min and run time, 43.87 min.

Table 3. Mass to charge ratio (m/z) of different fragments of nine analytes (HKs and HALs)

Analytes	Formula	Characteristic m/z Ions	
		Quantification Ions	Target Ions
Chloroacetone	CP	43	77, 92
1,1-dichloropropanone	DCP	43	63, 83
1,1,1-trichloropropanone	TCP	125	83, 97, 127
1,1,3,3,-TeCP	TeCP	83	85, 111, 113
Chloralhydrate	CH	82	83, 84, 85
Bromochloroacetaldehyde	BCAL	130	74, 79, 92
Dibromoacetaldehyde	DBAL	174	79, 81, 95, 172
Dibromochloroacetaldehyde	DBCAL	129	79, 81, 91, 93
Tribromoacetaldehyde (Bromal)	TBAL	173	81, 91, 171, 175
Dichloroacetaldehyde	DCAL	84	86, 112

3.2.4 Dissolved organic matter (DOC)

The dissolved organic matter concentration of the water samples was measured by using a Shimadzu TOC-Vws total organic carbon (TOC). The DOC analysis was carried out by using 30 mL of the filtered water sample into a 40 mL DOC vial and spiking two drops of hydrochloric acid (HCl) to the sample. The DOC measurement was carried out after filtering samples through a MicronSepNitrocelluloso 47 mm 0.45 µm membrane.

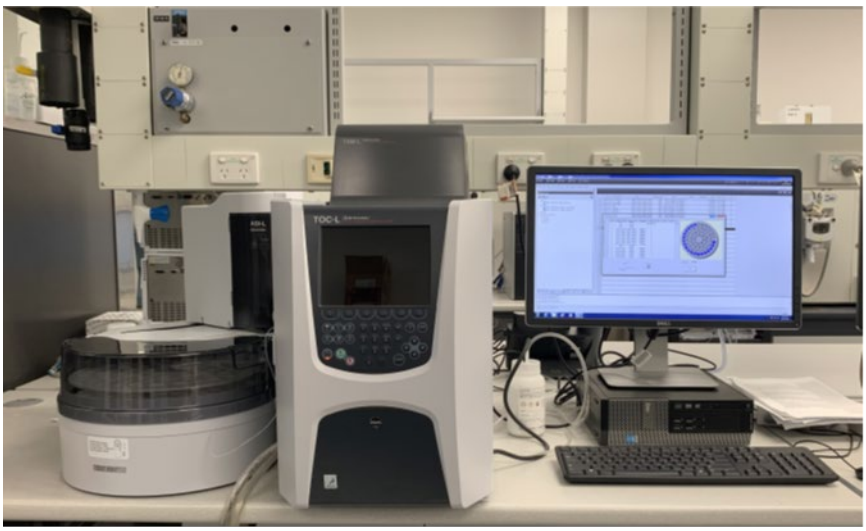

Figure 3. TOC analyser

681 ***3.2.5 UV_{254nm} absorbance measurements***

682 The UV absorbance of the water was measured at 254 nm by using a Cary 60 UV-Vis,
683 Agilent Technologies). The UV_{254nm} measurement was carried out after filtering sam-
684 ples through a MicronSepNitrocelluloso 47 mm 0.45 µm membrane.

685 ***3.2.6 Adsorbable Organic Halogen (AOX)***

686 The adsorbable organic halogen (AOX) content was analysed to identify and quantify
687 specific adsorbable organic halogens, i.e., AOCl, AOBr, and AOI, in drinking water
688 samples. Three chemicals, 1-chlorophenol, 4-bromophenol, and 4-iodophenol, were
689 used to prepare the calibration standards (Kristiana, McDonald, Tan, Joll, & Heitz,
690 2015; Markus Langsa Sebastien Allard Ina Kristiana Anna Heitz Cynthia, 2017; P. A.
691 Neale et al., 2012). All stock solutions (1-chlorophenol, 4-bromophenol and 4-iodo-
692 phenol) were prepared at a final concentration of 1 g/L in MeOH, separately. A work-
693 ing solution (10 mg/L) was prepared by adding the desired volume of all three analytes
694 into ultrapure water. Then, all standard solutions were prepared by spiking the appro-
695 priate volume of working solution into ultrapure water. The calibration standards con-
696 centrations were ranging from 0 to 500 µg/L. The unknown concentration of AOX in
697 the water samples was expected to be in this range.

698 The AOX method consisted of four steps: extraction, combustion, collection, and anal-
699 ysis. The organic halogens are adsorbed on active carbon during the extraction process.
700 50 mL water sample was extracted by passing through two activated carbon microcol-
701 umns in series using a Mitsubishi TOX sample preparatory (Model TX-3AA;
702 Mitsubishi, Japan). Then, the activated carbon columns were washed with 5 mL nitric
703 acid (HNO_3) solution (5 g/L). The nitric acid wash allows removing the inorganic hal-
704 ides from the activated carbon columns. After the HNO_3 wash, the activated carbon
705 was removed from the two microcolumns and transferred into a sample boat. Then the
706 sample boat was placed in an automatic solid sampler unit. Next, the boat was trans-
707 ferred to the combustion unit using an automatic quick furnace (AQF-100) Mitsubishi,
708 Japan for combustion at 1000 ˚C. During the combustion process, the AOX adsorbed
709 on the activated carbon are burned and a hydrogen halide gas (HX) is released. A mix
710 of argon gas with a flow rate of 200 mL/min and oxygen (O_2) with a flow rate of 400
711 mL/min are supplied to the inner pyrolysis tube to carry the HF formed. The HX gas
712 is then directed to the absorption unit which is filled with ultrapure water allowing the
713 HF to dissolved and formed the respective halogen ions (X^-). Finally, the solution

containing the halide ions is automatically injected in the ion Chromatography system ICS-3000, Dionex, Sunnyvale, CA, USA, and the different halogens are identified and quantified. Separation of halogenated organic ions was carried with an IonPac AS19, IC column 4 x 250 mm and with an IonPac AG19, guard column 4 x 50 mm (Dionex). A conductivity detector (Dionex ICS-3000 VWD) was used to detect halides.

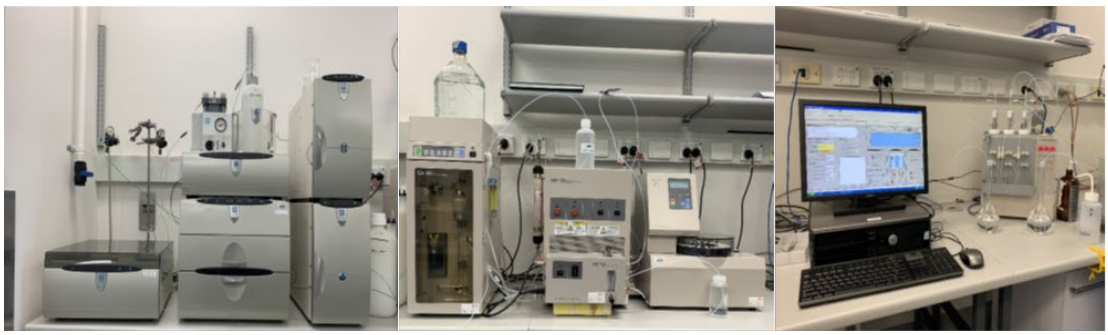

Figure 4. Mitsubishi TOX sample preparatory (Model TX-3AA; Mitsubishi, Japan), Automatic quick furnace (AQF-100) Mitsubishi, Japan, and ion Chromatography system ICS-3000, Dionex, Sunnyvale, CA, USA.

3.2.7 Ion chromatography (IC)

Ion chromatography was used to measure inorganic anions, i.e, chlorite (ClO_2^-), chlorate (ClO_3), bromate (BrO_3^-), and bromide (Br^-) simultaneously using a Dionex ICS3000 (AG9HC/AS9HC) system and a post-column reaction based on a previously published method (Salhi & von Gunten, 1999). Sodium chlorite ($NaClO_2$), sodium chlorate ($NaClO_3$), sodium bromate (NaBr), and sodium bromate ($NaBrO_3$) were used in this study for the calibration standards. 1 g/L stock solutions were prepared separately for all analytes into ultrapure water. 10 mg/L working solution was prepared by dilution of each solution in ultrapure water. Then, a sequence of calibration standards for Br^- from 0 µg/L to 500 µg/L was prepared by adding the desired volume of working solution to the ultrapure water. Similarly, a range of calibration standards from 0 µg/L to 50 µg/L was prepared for ClO_2^-, ClO_3^-, and BrO_3^- by spiking the desired volume. A sequence of calibration standards was prepared for ClO_2^-, ClO_3^-, BrO_3^- and Br^- with an appropriate range of concentrations, the unknown concentration of ions lie within the range.

3.3 Experimental Apparatus

3.3.1 Collimated-beam UV (CBD-UV)

UV treatment was carried out using CBD-UV irradiation from a low-pressure lamp (emitting at 254 nm) similar to the system described and published by Bolton and Linden (2003). The CBD-UV device contains three low-pressure (15 W) Hg UV-lamps

(UV Technik Meyer, Germany). The collimating tube extends from the lamps to collimate the UV light (Kuo, Chen, & Nellor, 2005). A magnetic stirrer and XY-cross slide table were placed below the collimator. The UV light intensity was measured using a radiometer (UV-surface-D, sglux, Germany) (Nihemaiti et al., 2018). The CBD-UV was turned on 30 min before the experiment every day to warm up the UV lamp and achieve a constant intensity. Then, the UV intensity was measured and recorded. The UV intensity was between 8.60 W/m^2 to 8.20 W/m^2. The UV intensity was used to determine the duration of the irradiation to achieve the desired UV dose or fluence for each experiment. The distance of the solution (water sample) from the UV lamp was 29 cm. During the UV irradiation, the solution was stirred by a magnetic stirrer at 400 rpm.

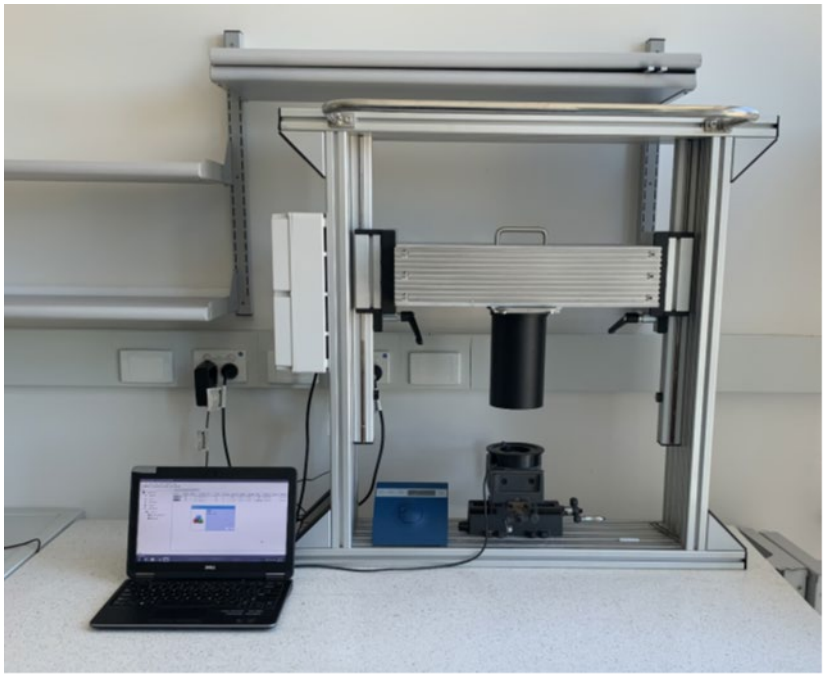

Figure 5. Collimated-beam UV (CBD-UV) system

3.4 Experimental Procedures

3.4.1 Chlorination treatment

The chlorine concentration of the commercial solution was measured by direct UV measurement at 292 nm using a molar extinction coefficient (ε) of 362 ± 5 (L/mol/cm). Thereafter, a 1 g/L chlorine stock solution was prepared. The 60 mL water sample was spiked with the desired volume of chlorine stock solution to achieve appropriate

762 chlorine concentration in the sample. The water sample was kept in the dark at room
763 temperature for an appropriate reaction time.

764 ***3.4.2 UV/ chlorine treatment***

765 UV/chlorine treatment was performed using the CBD-UV irradiation set up described
766 above. The duration of UV irradiation was calculated based on UV intensity to achieve
767 the desired fluence (UV dose). Water samples (60 mL) were placed in a petri dish and
768 exposed to UV irradiation for the desired fluences. The water sample was spiked with
769 the desired volume of chlorine solution and exposed to UV irradiation at the same
770 time. After reaching the UV dose, the water samples were transferred into 100 mL
771 amber bottles and kept in the dark at room temperature for a pre-determined reaction
772 time for reaction with the residual chlorine.

773 ***3.4.3 Procedure***

774 The water samples from MWTP and CMPP were used to assess and compare the for-
775 mation of DBPs during "dark chlorination" and UV/chlorine treatments under the fol-
776 lowing conditions. All the experiments were carried out at room temperature (17-22
777 °C). A 60 mL water sample was used in every experiment. The chlorine concentration
778 was 8 mgCl_2/L or 10 mgCl_2/L in all experiments for MWTP and CMPP, respectively.
779 Two UV doses of 1000 and 2000 mJ/cm^2, were applied to CMPP water samples, and
780 only 1000 mJ/cm^2 was applied to MWTP water samples. The CMPP water samples
781 were analysed at three different reaction times: 20 min, 40 min, and 24 h. The reaction
782 time was 24 h for all experiments performed using MWTP samples. Once the reaction
783 was completed, the chlorine residual was measured. Iodometric titration was used to
784 measure the chlorine residual by UV-Vis at 351 nm using epsilon 25700 L/mol/cm (S.
785 Allard, Fouche, Dick, Heitz, & von Gunten, 2013). Moreover, chlorine residual, DOC,
786 and UV_{254nm} were measured using UV-Vis immediately after the desired UV dose was
787 achieved and after treatments. Once the UV/ chlorine and chlorination treatments were
788 finished, all water samples were quenched with Na_2SO_4 reagent, and the pH, AOX,
789 inorganic ions, and DBPs analysis were carried out immediately. A series of standard
790 solutions with known concentrations were prepared to identify and quantify an analyte
791 in a water sample. Furthermore, the fragmentation pattern of each analyte was used to
792 qualitatively assess the presence of a compound. In a given mass spectrum, the ratio
793 between the quantitation ions and the targeted ion presented in table 1-3 (m/z) were
794 used as well as the retention time to identify an analyte.

Chapter 4: Results and Discussion

4.1 Variation of pH during UV/chlorination and dark chlorination

The pH was measured before and after dark chlorination and UV/chlorine oxidation. Figure 6 shows the pH of the untreated, chlorinated, and UV/chlorinated samples at the different stages of MWTP.

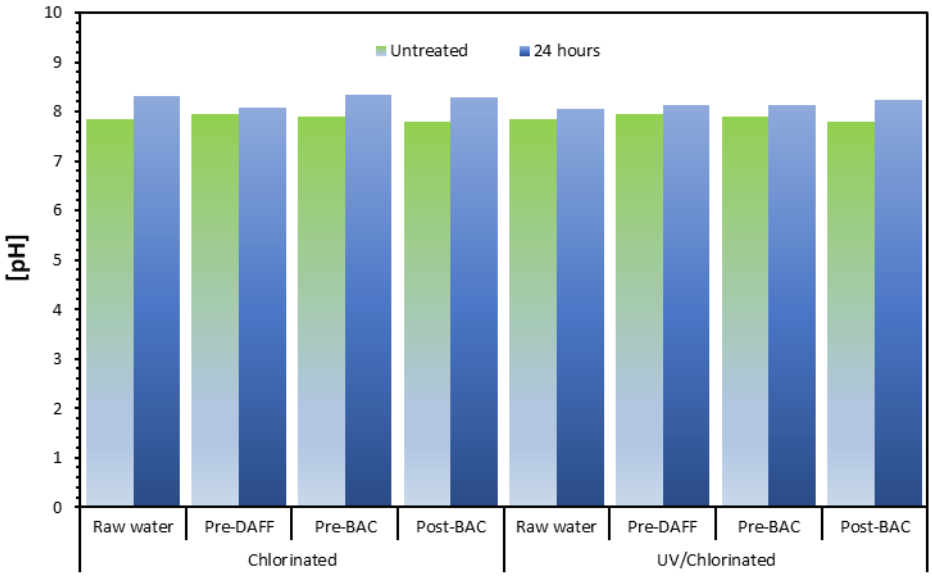

Figure 6. pH value for samples collected at a different stage of the MWTP before and after dark chlorination and UV/chlorine exposure. $[HOCl]_0$ 8 $mgCl_2/L$, 24 h contact time, UV dose of 1000 mJ/cm^2.

Figure 6 shows the pH of the water at a different stage of the MWTP before and after treatments. It can be observed in Figure 6 that the pH of all water samples slightly increased after treatments (24 h) during UV/chlorine oxidation (1000 mJ/cm^2) and dark chlorination compared to the untreated water samples. This is explained by the addition of chlorine (NaOCl) which is a basic solution. Therefore, the pH increase since OCl^- is consuming some proton H^+ through the equilibrium $OCl^- + H^+ \Leftrightarrow HOCl$.

Figure 6 shows that the pH of untreated raw water, pre-DAFF, pre-BAC, and post BAC water samples was 7.86, 7.96, 7.89, and 7.79, respectively. The pH of chlorinated water samples after 24 h in raw water, pre-DAFF, pre-BAC and post BAC water samples was 8.32, 8.08, 8.33, and 8.28, respectively. The pH of UV/chlorinated (1000 mJ/cm^2) water samples after 24 h in raw water, pre-DAFF, pre-BAC and post BAC water samples was 8.06, 8.12, 8.13, and 8.23, respectively. Figure 6 shows that the pH increased more during dark chlorination than in UV/chlorine oxidation (1000 mJ/cm^2)

except in the pre-DAFF water sample. This could probably be explained by the addition of the basic chlorine solution and additional consumption of chorine by UV photolysis.

4.2 Comparison between UV/chlorine and dark chlorination on NOM

Figure 7 shows the DOC concentration in the untreated, chlorinated, and UV/chlorinated samples after 24 h at the different stages of the water treatment train.

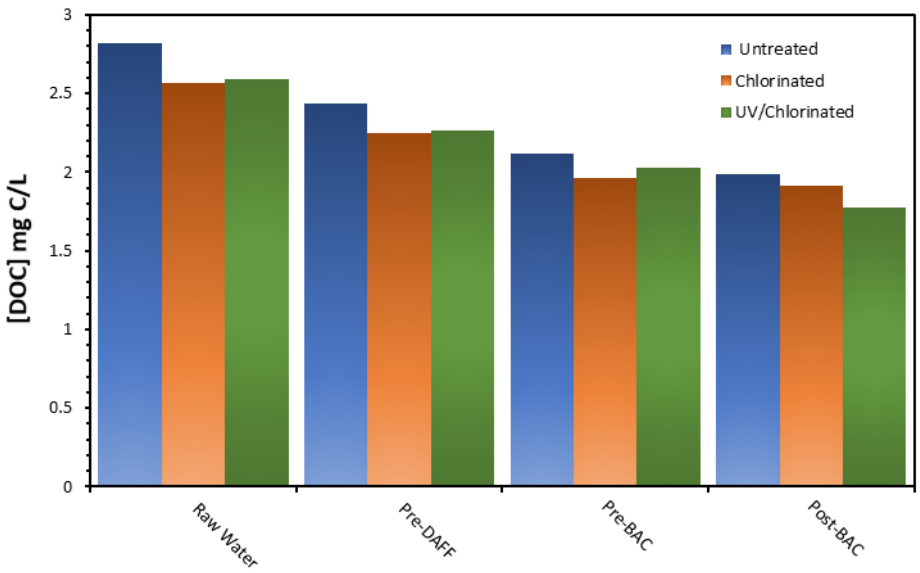

Figure 7. DOC content for samples collected at a different stage of the MWTP before and after dark chlorination and UV/chlorine exposure. $[HOCl]_0$ 8 $mgCl_2/L$, 24 h contact time, UV dose of 1000 mJ/cm^2.

As expected, the concentration of DOC decreased through the water treatment process. The raw water had the highest concentration of DOC with 2.8 mgC/L followed by pre-DAFF with 2.4 mgC/L, pre-BAC with 2.1 mgC/L, and post-BAC with 2.0 mgC/L. The analysis of the water samples after oxidative treatment shows that the concentration of DOC was decreased similarly by 9 % in dark chlorination and UV/chlorine oxidation for all samples. The DOC concentration decreased after dark chlorination with 2.6 mgC/L for the raw water, followed by pre-DAFF with 2.3 mgC/L, pre-BAC with 2.0 mgC/L, and post-BAC with 1.9 mgC/L. The DOC concentration was similarly reduced during UV/chlorine oxidation with 2.6 mgC/L for the raw water, followed by pre-DAFF with 2.3 mgC/L, pre-BAC with 2.0 mgC/L, and post-BAC with 1.8 mgC/L. Moreover, no significant change in DOC concentration was observed in UV/chlorine oxidation (1000 mJ/cm^2) compared to dark chlorination (Figure 7). This is similar to

Chow, et al. (2008) which observed that there was no noticeable change in DOC concentration after UV irradiation of surface water. According to the results, there were no significant differences between dark chlorination and UV/chlorination, and the difference in DOC between untreated and treated samples is coming from the formation of volatile compounds. Since they are volatile, they disappear, and therefore the DOC is lower.

Specific UV absorbance (SUVA) is defined as the UV absorbance of a water sample at a given wavelength (usually 254 nm) normalized by the DOC concentration (Weishaar et al., 2003). SUVA is usually used as a surrogate for NOM reactivity. A high SUVA is regarded as a high DBPs formation potential (L.-C. Hua, Chao, Huang, & Huang, 2020; Weishaar et al., 2003). Figure 8 shows the $SUVA_{254nm}$ in the untreated, chlorinated, and UV/chlorinated samples after 24 h at the different stages of the water treatment train. The $SUVA_{254nm}$ values were decreasing from the untreated to the treated samples. Interestingly and opposite to the DOC concentration reported above, a large difference was observed between the dark chlorination and UV/chlorine oxidation experiments for the $SUVA_{254nm}$ values.

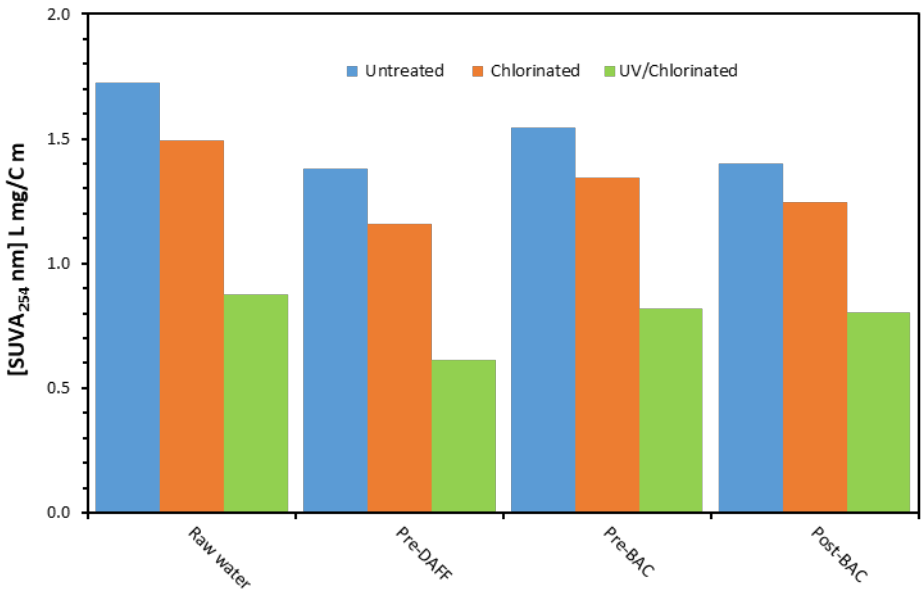

Figure 8. $SUVA_{254}$ value for samples collected at different stages of the MWTP before and after dark chlorination and UV/chlorine treatment. $[HOCl]_0$ 8 $mgCl_2/L$, 24 h contact time, UV dose of 1000 mJ/cm^2.

The $SUVA_{254nm}$ values for the raw water, pre-DAFF, pre-BAC and post-BAC were1.7 $L.mg.C^{-1}.m^{-1}$, 1.4 $L.mg.C^{-1}.m^{-1}$, 1.5 $L.mg.C^{-1}.m^{-1}$and 1.4 $L.mg.C^{-1}.m^{-1}$, respectively. The $SUVA_{254nm}$ value after dark chlorination for raw water, pre-DAFF, pre-BAC and

post-BAC were 1.5 $L.mg.C^{-1}.m^{-1}$, 1.2 $L.mg.C^{-1}.m^{-1}$, 1.3 $L.mg.C^{-1}.m^{-1}$and post-BAC: 1.2 $L.mg.C^{-1}.m^{-1}$, respectively. The $SUVA_{254nm}$ value after UV/chlorine treatment in raw water, pre-DAFF, pre-BAC and post-BAC were 0.9 $L.mg.C^{-1}.m^{-1}$, 0.6 $L.mg.C^{-1}.m^{-1}$, 0.8 $L.mg.C^{-1}.m^{-1}$ and 0.8 $L.mg.C^{-1}.m^{-1}$ after 24 h, respectively.

It can be observed that the $SUVA_{254nm}$ values significantly decreased during UV/chlorine oxidation compared to the dark chlorination with an average of 50.0% and 20.1%, respectively. For example, the $SUVA_{254nm}$ value in the raw water untreated, chlorinated, and UV/chlorinated was 1.7 $L.mg.C^{-1}.m^{-1}$, 1.5 $L.mg.C^{-1}.m^{-1}$ and 0.9 $L.mg.C^{-1}.m^{-1}$, respectively. A similar trend was observed for the pre-DAFF, pre-BAC, and post-BAC water samples. Similar results were observed in previous studies by Chow et al. (2008) and Lee et al. (2014).

The changes in $SUVA_{254nm}$ values showed that the NOM structure is changing during UV irradiation. Some aromatic chromophores were destroyed by UV irradiation and some aromatic compounds were oxidised by chlorine. The formed by-products were not absorbing UV irradiation (Chu, Gao, Krasner, Templeton, & Yin, 2012; Hur, 2011). This has important implications since, unlike common practice where a decrease in $SUVA_{254nm}$ is associated with a lower NOM reactivity and therefore a lower formation of DBPs, a higher formation of DBPs have been observed after UV/chlorination even though a decrease in $SUVA_{254nm}$ was observed (Wei Liu et al., 2006). According to Wang et al., (2017) reactive radicals $OH^{\bullet}$, $O^{\bullet-}$ and chlorine reactive species (CRSs) such as $Cl^{\bullet}$ and $Cl_2^{\bullet-}$ formed during the UV/chlorine advance oxidation process might form some DBPs precursors.

4.3 Impact of UV/chlorine treatment on chlorine consumption and comparison with dark chlorination

Figure 9 shows the chlorine concentration after UV/chlorine oxidation with a fluence of 1000 and 2000 mJ/cm^2, and dark chlorination at different reaction times of 20 min, 40 min, and 24 h.

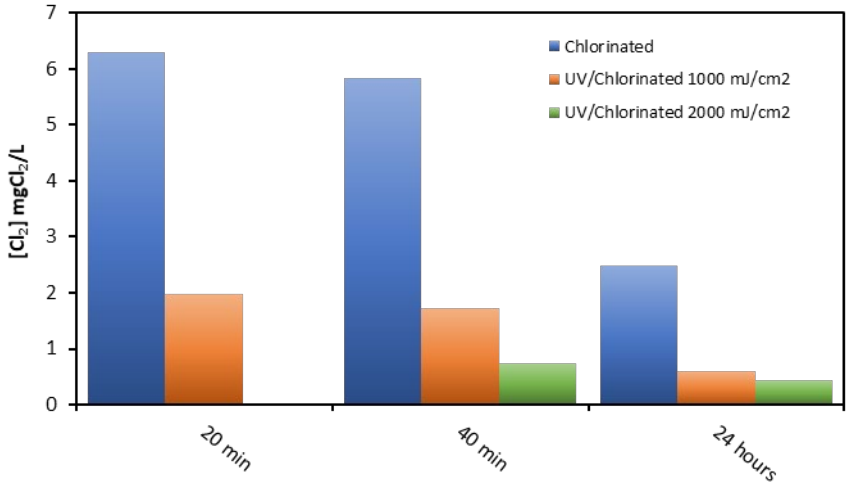

Figure 9. Chlorine residual after UV/chlorine oxidation with a fluence of 1000 and 2000 mJ/cm^2 and dark chlorination. $[HOCl]_0$ 10 mgCl_2/L.

Figure 9 shows that the chlorine concentration was decreased continuously during dark chlorination from 10 mgCl_2/L to 6.3 mgCl_2/L at 20 min, 5.8 mgCl_2/L at 40 min, and 2.5 mgCl_2/L after 24 h in the CMPP water. The degradation of chlorine was increased by increasing the UV dose from 1000 mJ/cm^2 to 2000 mJ/cm^2 (Figure 9). The chlorine concentration was greatly impacted by UV treatment. The chlorine decay was higher during UV/chlorine oxidation compared to dark chlorination with 2 mgCl_2/L at 20 min (there is no data for 2000 mJ/cm^2 since the irradiation was not completed), 1.7 mgCl_2/L and 0.7 mgCl_2/L at 40 min, and 0.6 mgCl_2/L and 0.4 mgCl_2/L after 24 h, for 1000 mJ/cm^2 and 2000 mJ/cm^2, respectively (Figure 9).

Similarly, Figure 10 shows that the concentration of chlorine was decreased during UV/chlorine oxidation with a fluence of 1000 mJ/cm^2 compared to dark chlorination for the MWTP samples.

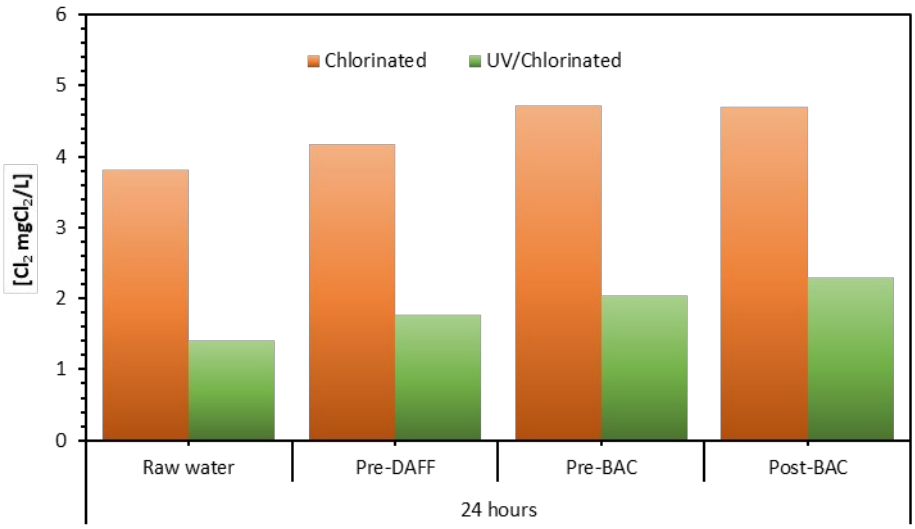

Figure 10. Chlorine residual measurement after UV/chlorine oxidation with a fluence of 1000 mJ/cm^2 and dark chlorination. In both experiments, chlorine concentration and reaction time were $[HOCl]_0$ 8 mgCl_2/L and 24 h, respectively.

Figure 10 shows that the concentration of chlorine was decreased during dark chlorination in raw water, pre-DAFF, pre-BAC, and post-BAC from 8.0 mgCl_2/L to 3.8 mgCl_2/L, 4.2 mgCl_2/L, 4.7 mgCl_2/L, and 4.7 mgCl_2/L after 24 h, respectively. Similarly, the chlorine concentration was decreased during UV/chlorine oxidation (1000 mJ/cm^2) in raw water, pre-DAFF, pre-BAC and post-BAC from 8.0 mgCl_2/L to1.4 mgCl_2/L, 1.8 mgCl_2/L, 2 mgCl_2/L and 2.3 mgCl_2/L after 24 h, respectively. It is clear from Figure 10 that the chlorine degradation was much higher in UV/chlorine oxidation than in dark chlorination with 63% more degradation for the raw water sample.

4.4 The behavior of inorganic species during UV/chlorine oxidation and dark chlorination

In these experiments, bromate and chlorite were not detected. The only chlorate was detected. Figure 11 shows that the concentration of chlorate was gradually increasing after UV/ chlorine oxidation with a fluence of 1000 mJ/cm^2 in raw water, pre-DAFF, and post-BAC water samples after 24 h while the pre-BAC water sample had the lowest formation compared to the raw water.

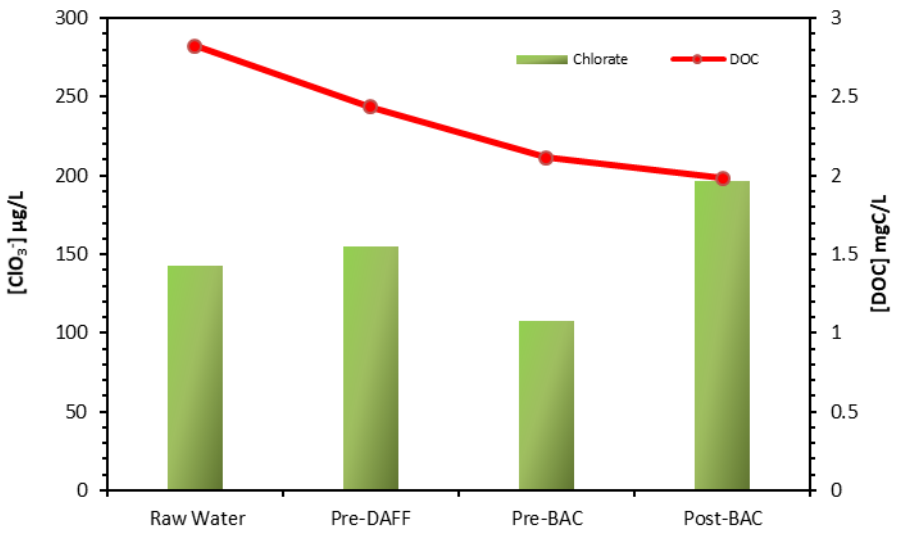

Figure 11. Chlorate concentration for samples collected at different stages of the MWTP before and after dark chlorination and UV/chlorine exposure. $[HOCl]_0$ 8 mgCl_2/L, 24 h contact time, UV dose of 1000 mJ/cm^2.

Figure 11 shows that the chlorate concentration of raw water, pre-DAFF, pre-BAC, and post-BAC water samples was 142.4 µg/L, 155.1 µg/L, 107.4 µg/L, and 196.4 µg/L, respectively. This is inversely correlated to the DOC concentration. Since the DOC decreased along the treatment train there is less competition between organic and inorganic species to react with the radical species formed during the UV/chlorine process and therefore more chlorate is formed.

4.5 Adsorbable organic halogen (AOX) formation during UV/chlorine oxidation and dark chlorination

4.5.1 Total AOX formation in CMPP water samples

Figure 12 shows the formation of AOCl, AOBr, and total AOX concentration after UV/chlorine oxidation with a fluence of 1000 and 2000 mJ/cm^2, and dark chlorination at different reaction times 20 min, 40 min, and 24 h in the CMPP water.

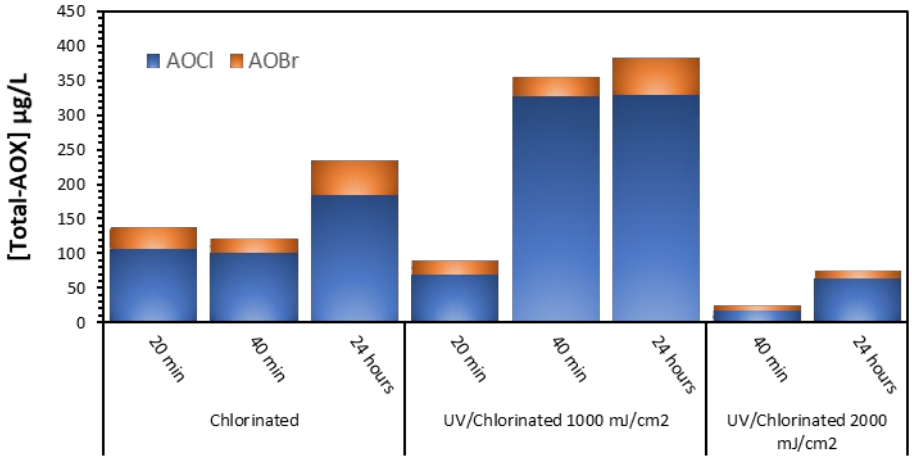

Figure 12. AOBr and AOCl concentration after UV/chlorine oxidation with a fluence of 1000 and 2000 mJ/cm^2 and dark chlorination. $[HOCl]_0$ 10 mgCl_2/L.

As expected, the total AOX formation was increasing with increasing contact time with the oxidant. However, significant differences were observed between dark chlorination and UV/Chlorine experiments at different UV doses. The concentration of AOCl after 20 min was higher for the dark chlorination experiments with 105.9 µg/L compared to the UV/Chlorine experiments at 1000 mJ/cm^2 with 68.9 µg/L. A different pattern was observed at 40 min and 24 h with 100.5 µg/L and 184.1 µg/L for the dark chlorination, a higher concentration of 327.5 µg/L and 328.3 µg/L for the UV dose of 1000 mJ/cm^2 and a lower concentration of 18.0 µg/L and 62.8 µg/L for the UV dose of 2000 mJ/cm^2, respectively. Similarly, Figure 12 shows that the concentration of AOBr after 20 min was higher for the dark chlorination experiments with 32.4 µg/L compared to the UV/Chlorine experiments with 21.2 µg/L. A different pattern was observed at 40 min and 24 h with 20.7 µg/L and 50.6 µg/L for the dark chlorination, a higher concentration of 28.3 µg/L and 54.1 µg/L for the UV dose of 1000 mJ/cm^2 and a lower concentration of 7.0 µg/L and 12.8 µg/L for the UV dose of 2000 mJ/cm^2,

respectively. In this case, the choice of the UV dose is critical to mitigating the AOX formation.

4.5.2 Total AOX formation in MWTP water samples

Figure 13 shows the formation of AOCl, AOBr and total AOX concentration in chlorinated and UV/chlorinated samples after 24 h at the different stages of the water treatment train.

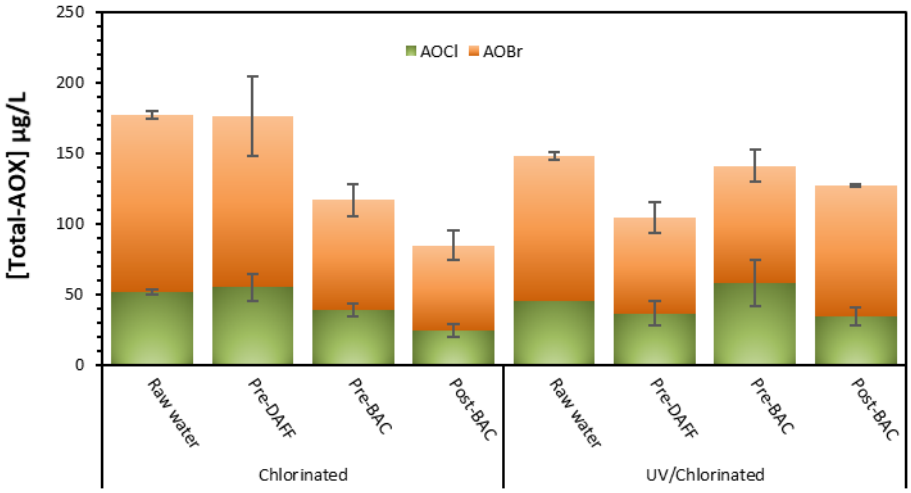

Figure 13. AOBr and AOCl concentrations after UV/chlorine oxidation with a fluence of 1000 mJ/cm^2 and dark chlorination. $[HOCl]_0$ 8 mgCl_2/L and 24 h.

Figure 13 shows that the total AOX formation from dark chlorination decreased along the treatment train from 177.0 µg/L to 84.8 µg/L similar to the DOC concentration (Figure 7) while for the UV/chlorine experiment the AOX formation trend is different with a decrease from the raw water (148.0 µg/L) to the pre-DAFF (104.8 µg/L) and an increase from the pre-DAFF to the pre-BAC (141.2 µg/L) and post-BAC (127.5 µg/L). This trend is similar to the $SUVA_{254nm}$ (Figure 8). It is interesting to notice that the formation of AOX was lower during UV/chlorine treatment with 148.0 µg/L and 104.8 µg/L compared to dark chlorination with 177.0 µg/L and 176.5 µg/L for the raw water and pre-DAFF samples while the opposite was observed for the pre-BAC and post-BAC where the formation of AOX was higher during UV/chlorine treatment with 141.2 µg/L and 127.5 µg/L compared to dark chlorination with 116.9 µg/L and 84.8 µg/L, respectively. In this particular case, UV/chlorine is not beneficial over dark chlorination. The same trend was observed when looking at individual AOX, i.e. AOCl and AOBr. However, AOBr was found at a much higher concentration than AOCl,

AOBr accounts for 68.0 to 70.8 % of the total AOX of raw water in UV/chlorination and dark chlorination treatments, respectively. In this case, the change in NOM characteristics induced by the different steps of the treatment train seems to be driving the AOX formation.

4.6 Comparison of the formation of Disinfectant by-products (DBPs) during UV/chlorine oxidation and dark chlorination

4.6.1 Trihalomethanes (THMs)

Figure 14 shows the formation of THMs during UV/chlorine oxidation with a fluence of 1000 and 2000 mJ/cm^2, and dark chlorination at different reaction times, 20 min, 40 min, and 24 h in the CMPP water.

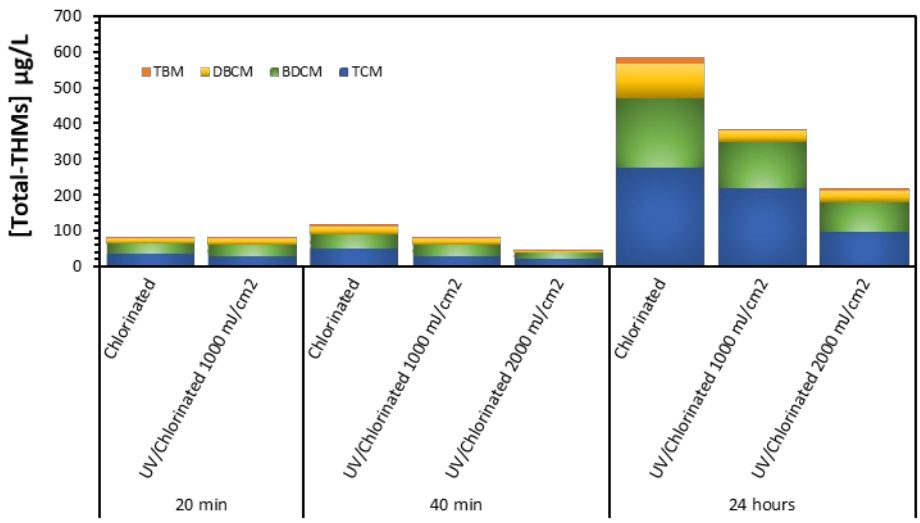

Figure 14. THMs formation after UV/chlorine oxidation with a fluence of 1000 and 2000 mJ/cm^2 and dark chlorination. $[HOCl]_0$ 10 mgCl_2/L.

As shown in Figure 14, the four THMs, i.e., TCM, TBM, BDCM, and DBCM were formed during both UV/Chlorine oxidation (1000 and 2000 mJ/cm^2) and dark chlorination, and their concentrations increased over time. The total concentration of THMs (TTHMs) was similar at 20 min reaction time with 82.5 µg/L and 81.2 µg/L for dark chlorination and UV/Chlorine experiment. At 40 min, the UV treatment had an impact and a decrease in TTHMs formation was observed with 118.1 µg/L for dark chlorination, 82.1 µg/L for 1000 mJ/cm^2 and 44.9 µg/L for 2000 mJ/cm^2. At 24h the TTHMs

were much higher but the same trend was observed with 584.5 µg/L for for dark chlorination,383.4 µg/L for 1000 mJ/cm^2 and 217.5 µg/L for 2000 mJ/cm^2. After 24 h, applying a UV dose of 2000 mJ/cm^2 mitigated the TTHMs formation by 62.8%. Reaction time is crucial, with more formation of TTHMs at 24 h. In general, the concentration of DBPs increases with contact time (Bulman & Remucal, 2020; Mercier Shanks, Sérodes, & Rodriguez, 2013). Formation of TTHMs decreased during UV/Chlorine oxidation (1000 and 2000 mJ/cm^2) compared to dark chlorination at 40 min and 24 h. During UV/Chlorine oxidation, the decrease in TTHMs concentration indicates that the reactive oxidants formed during chlorine photolysis are less efficient at generating THMs than in dark chlorination (Bulman & Remucal, 2020). Decreasing chlorine contact time from chlorine degradation through photolysis and radical chain reaction (Ben et al., 2016; Bulman & Remucal, 2020; Sun, Lee, Zhang, & Huang, 2016) and aromatic compounds removal (Sebastien Allard, Tan, Joll, & von Gunten, 2015; Heller-Grossman, Manka, Limoni-Relis, & Rebhun, 2001; Huang & Shah, 2018), limits THMs production.

With regards to the speciation of THMs, the same pattern was observed for all experiments with a higher formation of chlorinated THMs compared to brominated THMs in the order TCM>BDCM>DBCM>TBM. For examples at 24h contact time the concentration of TCM was 275.0 µg/L and 96.5 µg/L, BDCM 194.1 µg/L and 83.3 µg/L, DBCM 98.2 µg/L and 32.8 µg/L, TBM 17.2 µg/L and 5.0 µg/L for the dark chlorination and the 2000 mJ/cm^2 experiments, respectively. It is also interesting to notice that THMs and AOX exhibit different behavior and therefore it can be concluded that THMs are not a good surrogate for the total formation of halogenated organic compounds.

Figure 15 shows the formation of THMs at the different stages of the MWTP and the comparison between dark chlorination and UV/chlorine treatment at 1000 mJ/cm^2 after 24 h of contact time.

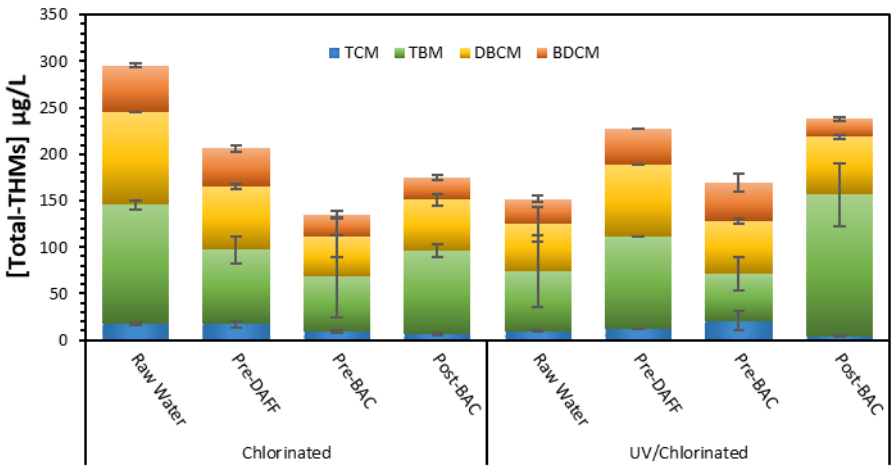

Figure 15. THMs concentration after UV/chlorine oxidation with a fluence of 1000 mJ/cm^2 and dark chlorination $[HOCl]_0$ 8 mgCl_2/L and 24 h..

As shown in Figure 15 the TTHMs decreased through the treatment train during chlorination (except for the post-BAC sample) similar to the DOC (Figure 7) and the AOX (Figure 13) concentration with 295.4 µg/L for the raw water and 134.8 µg/L for the pre-BAC. While for the UV/chlorine experiment the TTHMs formation trend is different with an increase from the raw water (151.9 µg/L) to the pre-DAFF (226.7 µg/L) and a decrease from the pre-DAFF to the pre-BAC (169.1 µg/L) and an increase from the pre-BAC to the post-BAC (237.8 µg/L). These results are opposite to previous results (Figure 14); TTHMs formation increased more with 1000 mJ/cm$_2$ and longer contact time (24 h) in all water samples except for the raw water sample. During UV/Chlorine oxidation, the increased in TTHMs concentration indicates that the reactive oxidants formed during chlorine photolysis are more efficient at generating THMs than in dark chlorination for pre-DAFF, pre-BAC and post-BAC. Furthermore, reactive chlorine species (RCS) may be involved in the formation of THMs. This trend is opposite to the AOX formation during UV/chlorine treatment (Figure 13).

The speciation of the THMs is different from the CMMP sample with a higher abundance of brominated THMs. For the dark chlorination experiments, the speciation of the THMs was not impacted by the different treatment applied, only the concentration was decreasing. For the UV/chlorine experiment, not only the TTHMs concentration but the concentration of highly brominated THMs is increasing along the treatment train with TCM decreasing from 9.5 µg/L to 4.2 µg/L, BDCM 27.2 µg/L to 19.4 µg/L,

DBCM increasing from 50.3 µg/L to 62.2 µg/L and TBM increasing from 64.9 µg/L to 152 µg/L for the raw water and the post-BAC, respectively.

4.6.2 Haloacetonitriles (HANs)

Figure 16 shows HANs formation during dark chlorination and UV/chlorine oxidation with a fluence of 1000 and 2000 mJ/cm^2 at different reaction times. Only DCAN and DBAN out of the 6 HANs analysed were detected in the samples.

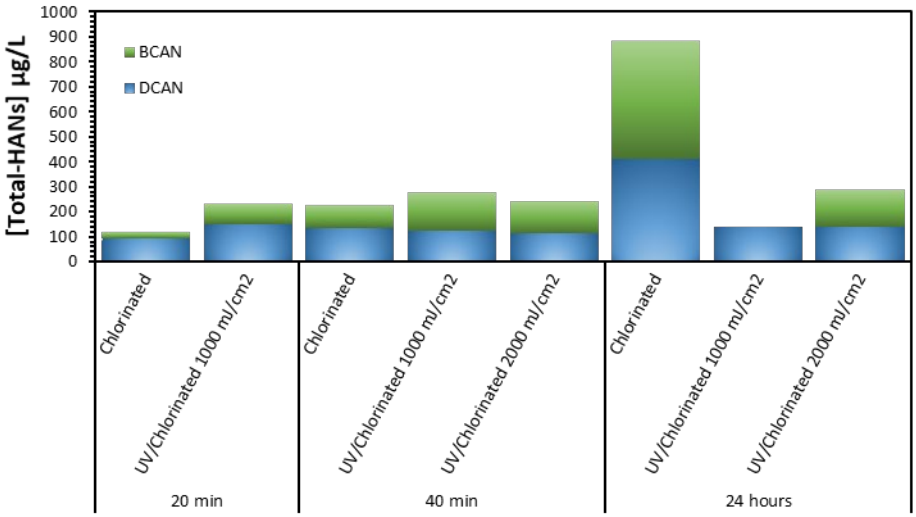

Figure 16. HANsconcentration after UV/chlorine oxidation with fluence of 1000 and 2000 mJ/cm^2 and dark chlorination. $[HOCl]_0$ 10 mgCl_2/L.

Figure 16 shows that the total concentration of DCAN and BCAN increased after UV/Chlorine treatment and 20 min contact time with 92.3 µg/L and 25 µg/L, respectively compared to 82.9 µg/L and 147.7 µg/L for the dark chlorination. At 40 min, the total concentration of DCAN was similar after dark chlorination (135.0 µg/L) compared to UV/chlorine at 1000 mJ/cm^2 and 2000 mJ/cm^2 with 123.5 µg/L and 113.5 µg/L, respectively. The formation of DCAN was decreased by increasing the UV dose from 1000 mJ/cm^2 to 2000 mJ/cm^2 (Figure 16). Similarly, the total concentration of BCAN was impacted by UV treatment with 149.3 µg/L after 24h contact time, the THANs is deeply mitigated by the UV/Chlorine treatment with 137.5 µg/L and 288.9 µg/L compared to 884.0 µg/L for the dark chlorination. Figure 16 suggests that THANs formation was impacted by increasing UV dose and contact time which means that HANs precursors were decayed in chlorine photolysis. Moreover, these results indicate that radical reactions mediated THANs formation. BCAN was surprisingly not detected at 24h for the1000 mJ/cm^2 experiments. This couldn't be explained and might be due to an analytical issue.

Figure 17 shows the formation of HANs in MWTP water samples during dark chlorination and UV/chlorine oxidation after 24 h. CAN, DCAN and BCAN were formed at different a stage of the water treatment plant both during dark chlorination and UV/chlorine oxidation.

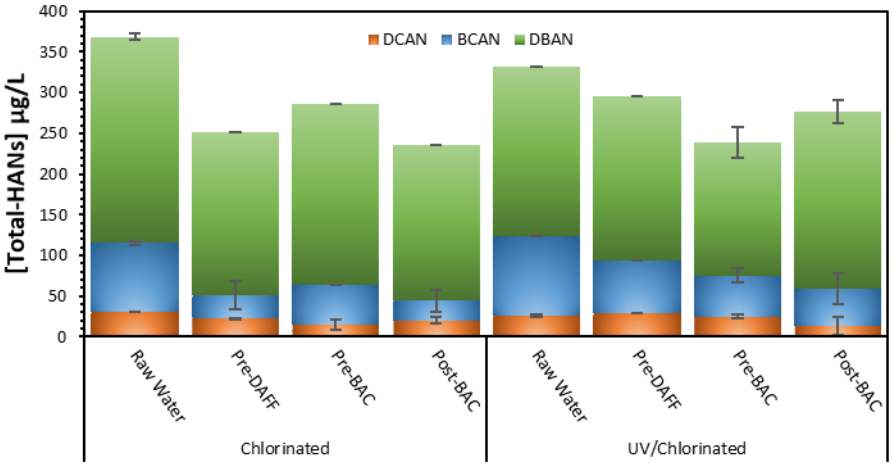

Figure 17. HANs concentration after UV/chlorine oxidation with a fluence of 1000 mJ/cm^2 and dark chlorination. $[HOCl]_0$ 8 mgCl_2/L and 24 h.

Figure 17 shows that the formation of DCAN, BCAN, and DBAN is decreasing through the water treatment train after chlorination with THANs formed at 368.8 µg/L in the raw water samples, 251.1 µg/L in the pre-DAFF, 286.7 µg/L in the pre-BAC, and 235.3 µg/L in the post-BAC. The application of UV decreased the THANs in the raw water and pre-BAC samples with 332.2 µg/L and 238.6 µg/L but an increase was observed for the pre-DAFF and post-BAC samples compared to dark chlorination with 296.2 µg/L and 276.5 µg/L. The speciation was dominated by DBAN followed by BCAN and low concentrations of DCAN for all experiments.

4.6.3 Haloacetic acids (HAAs)

Figure 18 shows the formation of HAAs during UV/chlorine oxidation with a fluence of 1000, and 2000 mJ/cm^2, and dark chlorination at different reaction times of 20 min and 24 h. Only DCAA and BCAA were detected after dark chlorination and UV/chlorine oxidation (1000 and 2000 mJ/cm^2). DBAA was detected only in one instance after UV/chlorine oxidation with a fluence of 1000 mJ/cm^2 at 20 min.

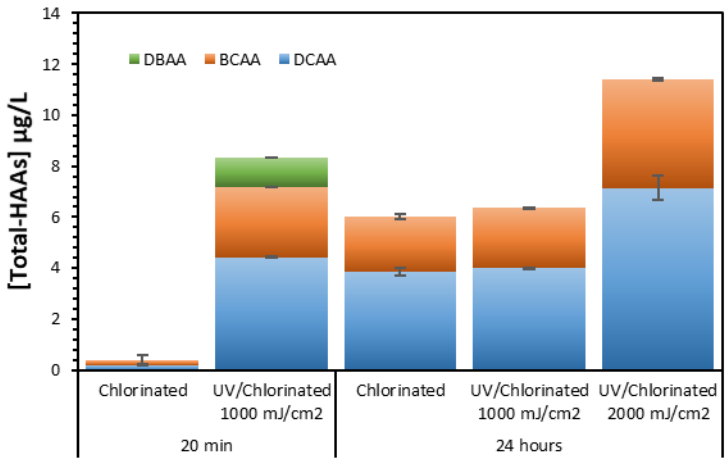

Figure 18. HAAs concentration after UV/chlorine oxidation with a fluence of 1000 and 2000 mJ/cm^2 and dark chlorination. $[HOCl]_0$ 10 mgCl_2/L.

As shown in Figure 18 the formation of DCAA and BCAA increased significantly during UV/chlorine oxidation compared to dark chlorination after 20 min and 24 h. The THAAs after 20 min in dark chlorination and UV/chlorine oxidation (1000 mJ/cm^2) was 0.4 µg/L and 8.3 µg/L, respectively. Similarly, the concentration of THAAs after 24 h increased from 6.0 µg/L in dark chlorination, to 6.4 µg/L for a UV dose of 1000 mJ/cm^2 and 11.4 µg/L for a UV dose of 2000 mJ/cm^2. This clearly showed that the impact of UV is detrimental to the mitigation of HAAs with 90% more THAAs after 2000 mJ/cm^2 of UV compared to dark chlorination. The speciation of HAAs was dominated by DCAA with for example 7.2 µg/L compared to 4.3 µg/L of BCAA after 24 h and UV chlorine treatment with a UV dose of 2000 mJ/cm^2. These results indicate that the RCS may be contributed in generating HAAs, due to chlorine consumption is much higher in UV/chlorine oxidation than in dark chlorination. Radicals such as RCSs produced during chlorine photolysis magnify HAA formation by interacting with HAA precursors (Gao et al., 2019).

Figure 19 shows that the total HAAs concentrationafter dark chlorination and UV/chlorine oxidation (1000 mJ/cm^2) decreased along the treatment train from 59.1 µg/L to 16.6 µg/L and 54.8 µg/L to 16.5 µg/L similar to the DOC concentration (Figure 7), respectively.

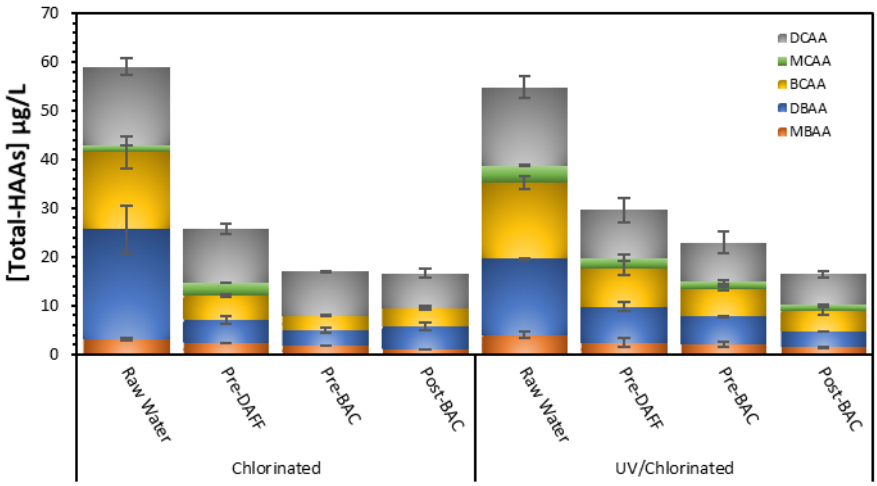

Figure 19. HAAs concentration after UV/chlorine oxidation with a fluence of 1000 mJ/cm^2 and dark chlorination. $[HOCl]_0$ 8 mgCl_2/L and 24 h.

Figure 19 shows that the THAAs concentration was decreased continuously through the treatment train during dark chlorination in raw water, pre-DAFF, pre-BAC, and post-BAC from 59.1 µg/L to 25.7 µg/L, 17.0 µg/L, and 16.6 µg/L after 24 h, respectively. Similarly, the THAAsconcentration was decreased continuously during UV/chlorine oxidation (1000 mJ/cm^2) in raw water, pre-DAFF, pre-BAC, and post-BAC from 54.8 µg/L to 29.6 µg/L, 22.9 µg/L and 16.5 µg/L after 24 h, respectively. It can be observed in Figure 19 that the THAAs concentration was decreased slightly during UV/chlorine oxidation (1000 mJ/cm^2) for raw water and post-BAC compared to dark chlorination whileTHAAs concentration was increased in pre-DAFF and pre-BAC samples after 24 h. These results suggest that the RCS may be contributed in generating HAAs. Nevertheless, the rise in HAAs concentration during chlorine photolysis might generate HAAs precursors from dissolved organic matter transformation because HAAs formation does not stop entirely by quenching (Bulman & Remucal, 2020). Overall, the use of UV/chlorine does not greatly impact the formation of THAAs.

MCAA, DCAA, BCAA, DBAA, and MBAA were formed in all water samples during dark chlorination and UV/chlorine oxidation (1000 mJ/cm^2) after 24 h. The speciation

of the HAAs is different from the CMMP sample with a higher abundance of brominated HAAs. For the dark chlorination experiments, the speciation of the HAAs was not impacted by the different treatment applied, only the concentration was decreasing. For the UV/chlorine experiment, not only the THAAs concentration but the concentration of highly brominated THAAs is increasing along the treatment train with BCAA decreasing from 15.7 µg/L to 4.2 µg/L, DBAA 15.6 µg/L to 3.3 µg/L, MBAA increasing from 4.0 µg/L to 1.4 µg/L for the raw water and the post-BAC, respectively.

4.6.4 Haloketones (HKs)

Figure 20 shows HKs formation during UV/chlorine oxidation with a fluence of 1000 and 2000 mJ/cm^2 and dark chlorination at different reaction times20 min, 40 min, and 24 h. Only 1,1- dichloropropanone (DCP) and 1,1,1- trichloropropanone (TCP) out of the 4HKs analysed were detected in the samples.

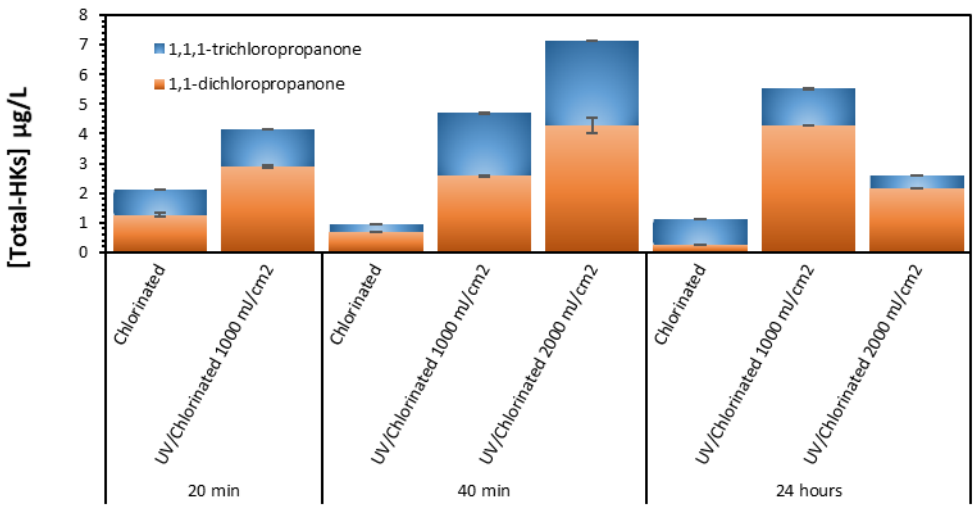

Figure 20. HKsconcentration after UV/chlorine oxidation with a fluence of 1000 and 2000 mJ/cm^2 and dark chlorination. [HOCl]$_0$ 10 mgCl$_2$/L.

As shown in Figure 20 the formation of DCP and TCP increased significantly during UV/chlorine oxidation compared to dark chlorination after 20 min, 40 min, and 24 h. The total concentration of DCP and TCP after 20 min in dark chlorination and UV/chlorine oxidation (1000 mJ/cm^2) was 2.1 µg/L and 4.2 µg/L, respectively. Similarly, the concentration of THKs after 40 min increased from 0.9 µg/L in dark chlorination, to 4.7 µg/L for a UV dose of 1000 mJ/cm^2 and 7.1 µg/L for a UV dose of 2000 mJ/cm^2. The abundance of THKs formed during UV/chlorine oxidation is higher than in dark chlorination, might be due to the decomposition (for example, Cl-substitution and Cl-addition reactions) of HKs precursors by reactive chlorine species (Alegre et

al., 2000; W.-L. Wang et al., 2017). The trend is different after 24 h with an increased concentration of THKs from dark chlorination (1.1 µg/L) to UV/chlorine at a dose of 1000 mJ/cm^2 (5.5 µg/L) and a decrease at a dose of 2000 mJ/cm^2 (2.6 µg/L). This clearly showed that the impact of UV is detrimental to the mitigation of HKs with 236.4% more THKs after 2000 mJ/cm^2 of UV compared to dark chlorination. The speciation of HKs was dominated by DCP with for example 2.1 µg/L compare to 0.4 µg/L of TCP after 24 h and UV chlorine treatment with a UV dose of 2000 mJ/cm^2.

Figure 21 shows the formation of HKs in MWTP water samples during dark chlorination and UV/chlorine oxidation after 24 h. Only TCP were formed at a different stage of the water treatment plant both during dark chlorination (except in post-BAC) and UV/chlorine oxidation while DCP was formed only in a raw water sample after dark chlorination.

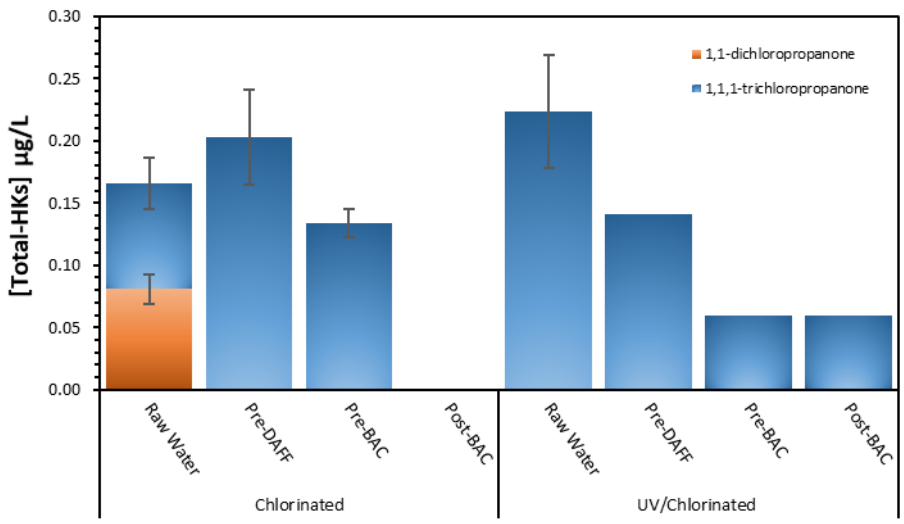

Figure 21. HKs concentration after UV/chlorine oxidation with a fluence of 1000 mJ/cm^2 and dark chlorination $[HOCl]_0$ 8 mgCl$_2$/L and 24 h.

During dark chlorination no clear trend was observed with 0.08 µg/L for DCP and TCP. There was an issue with the post-BAC sample and no data could be extracted. Figure 21 shows that the formation of TCP is decreasing through the water treatment train with 0.22 µg/L in the raw water samples, 0.14 µg/L in the pre-DAFF, 0.06 µg/L in the pre-BAC, and 0.06 µg/L in the post-BAC after UV/chlorine oxidation. The application of UV decreased the HKs in the pre-DAFF and pre-BAC samples but an increase was observed for the raw water samples compared to dark chlorination. The speciation was dominated by TCP for all experiments.

4.6.5 Haloacetaldehydes (HALs)

Figure 22 shows the formation of HALs during UV/chlorine oxidation with a fluence of 1000, and 2000 mJ/cm^2, and dark chlorination at different reaction times of 20 min, 40 min, and 24 h. Only CH and DCAL were detected after dark chlorination and UV/chlorine oxidation (1000 and 2000 mJ/cm^2). The total HALs formation was increasing with increasing contact time with the oxidant.

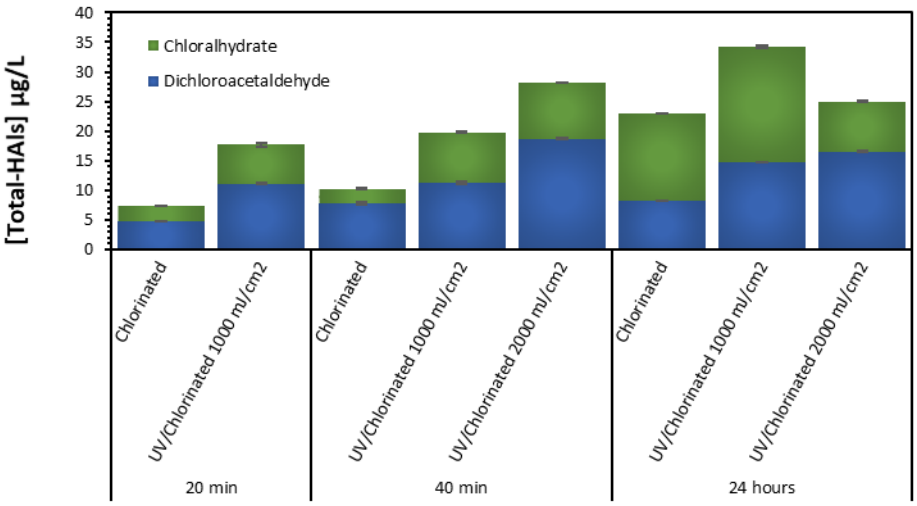

Figure 22. HALs concentration after UV/chlorine oxidation with a fluence of 1000 and 2000 mJ/cm^2 and dark chlorination. $[HOCl]_0$ 10 mgCl_2/L.

As shown in Figure 22 the concentration of CH and DCAL was higher during UV/chlorine oxidation compared to dark chlorination after 20 min, 40 min, and 24 h. The THALs after 20 min in dark chlorination and UV/chlorine oxidation (1000 mJ/cm^2) was 7.4 µg/L and 17.7 µg/L, respectively. Similarly, the concentration of THALs after 40 min increased from 10.3 µg/L in dark chlorination, to 19.8 µg/L for a UV dose of 1000 mJ/cm^2 and 28.2 µg/L for a UV dose of 2000 mJ/cm^2. The data indicate that THALs formation increase in the photolysis of chlorine at 20 min and 40 min relative to dark chlorination. The higher formation of THAls in UV/chlorine oxidation suggests that the reactive oxidant formed in chlorin photolysis enhance the formation of THALs. Furthermore, the results show that RCS may contribute to the evolution HALs and the HALs precursors are affected by the formation of RCS (Bulman & Remucal, 2020; Lyon et al., 2012). A different pattern was observed at 24 h with 23.0 µg/L for the dark chlorination, a higher concentration of 34.2 µg/L for the UV dose of 1000 mJ/cm^{2,} and a lower concentration of 25.0 µg/L for the UV dose of 2000 mJ/cm^2, respectively.

This clearly showed that the impact of UV is detrimental to the mitigation of HALs with 48.7% and 8.7% more THALs after 1000 and 2000 mJ/cm^2 of UV compared to dark chlorination. The speciation of HALs was dominated by DCAL with for example 16.5 µg/L compares to 8.5 µg/L of CH after 24 h and UV chlorine treatment with a UV dose of 2000 mJ/cm^2.

Figure 23 shows the formation of HALs in MWTP water samples during dark chlorination and UV/chlorine oxidation after 24 h. Only chloralhydrate and DCAL were formed at a different stage of the water treatment plant both during dark chlorination (except in post-BAC and post-BAC) and UV/chlorine oxidation.

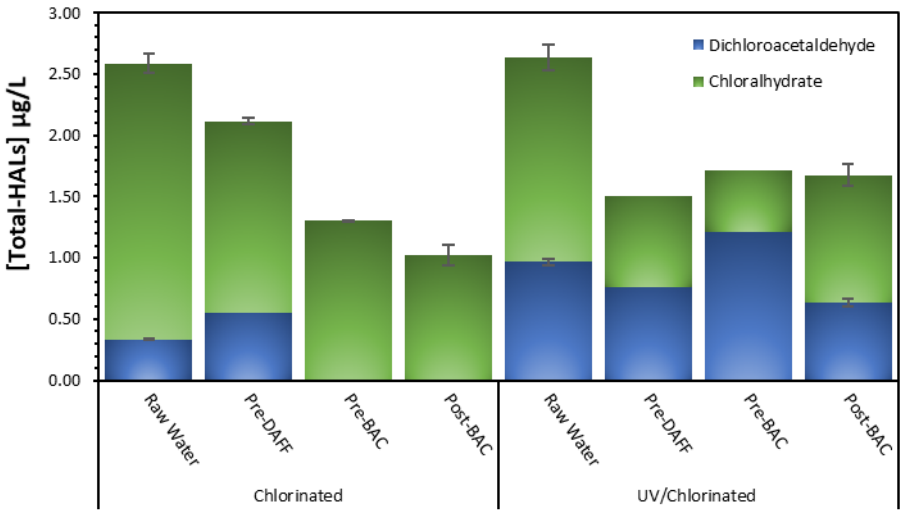

Figure 23. HALs concentration after UV/chlorine oxidation with a fluence of 1000 mJ/cm^2 and dark chlorination. $[HOCl]_0$ 8 mgCl_2/L and 24 h.

The concentration of THALs was decreasing along the treatment train for dark chlorination in raw water, pre-DAFF, pre-BAC, and post-BAC from 2.6 µg/L to 2.1 µg/L, 1.3 µg/L, and 1.0 µg/L after 24 h, respectively. While for the UV/chlorine experiment the THALs formation trend is different with a decrease from the raw water (2.6 µg/L) to the pre-DAFF (1.5 µg/L) and an increase from the pre-DAFF to the pre-BAC (1.7 µg/L) and the post-BAC (1.7 µg/L).

The application of UV decreased the CH in the raw water, pre-DAFF and pre-BAC samples with 1.7 µg/L, 0.7 µg/L and 0.5 µg/L but no change was observed for the post-BAC (1.0 µg/L) samples compared to dark chlorination with 2.2 µg/L, 1.6 µg/L, 1.3 µg/L and 1.0 µg/L, respectively. The data indicate that CH precursors are not affected by reactive oxidants formed in chlorin photolysis, which suggests that CRS production

during chlorine photolysis may not be involved in the formation of CH. According to WHO (1993), the concentration of CH is well below the provisional guideline (10 µg/L) in all water samples. However, the application of UV increased the DCAL in the raw water and pre-DAFF samples with 1.0 µg/L and 0.8 µg/L compared to dark chlorination with 0.3 µg/L and 0.6 µg/L, respectively. Moreover, the formation of the DCAL was observed during UV/chlorine oxidation in pre-BAC and post BAC samples with 1.2 µg/L and 0.6 µg/L while the formation of the DCAL was not observed during dark chlorination in pre-BAC and post BAC samples.

Chapter 5: Summary and Conclusions

The combination of ultraviolet (UV) irradiation and chlorination is regarded as a promising advanced oxidation process (AOP) to remove/reduce organic pollutants. However, predicting the formation of DBPs may become challenging as various factors influence the generation of halogenated DBPs such as UV fluence, type of lamp, NOM characteristics, chlorine dosage, and contact time during UV/chlorination. Several studies have been comparing the formation of DBPs from UV/chlorine with dark chlorination. However, contrasting results were reported.

Therefore, the main focus of this study was to undertake experiments with water samples exhibiting different reactivities collected from two different sources (MWTP and CMPP) to better understand the extent of DBPs formation during UV/chlorine treatment. THMs, HAAs, HANs, HALs, HKs, and AOX were analysed. A summary of the main output of this work is provided below:

5.1 NOM degradation and characteristics

The analysis of the water samples after oxidative treatment shows that the concentration of DOC decreased by 9% in dark chlorination and UV/chlorine oxidation without a noticeable difference between the two treatments. Interestingly and opposite to the DOC concentration, a significant difference was observed between the dark chlorination and UV/chlorine oxidation experiments for the $SUVA_{254nm}$ values which is used as a surrogate for NOM reactivity with oxidants. The $SUVA_{254nm}$ value significantly decreased during UV/chlorine oxidation compared to the dark chlorination with an average of 50.0% and 20.1%, respectively. The data imply that some aromatic chromophores were destroyed by UV irradiation, and some aromatic compounds were oxidised by chlorine. It is also possible that the aromatic structures of the dissolved organic matter samples, which were not contributed to producing DBPs were removed during the photooxidation process. These results suggest that UV/chlorination has the advantage in degrading NOM structure over dark chlorination in water with high DOC. Besides •OH, CRS are involved in the NOM degradation, which might form additional DBPs precursors and DBPs.

5.2 Chlorine residual

The final chlorine concentration was greatly impacted by the UV process when comparing dark chlorination to UV/HOCl. This is due to the fraction of chlorine which is photolysed by UV. Chlorinated and Hydroxyl radicals are produced at the same time during chlorine photolysis. However, it is hard to distinguish the role of each radical with regard to DBP precursor formation.

5.3 Chlorate formation

Chlorate are not formed during dark chlorination. However, the concentration of chlorate was gradually increasing after UV/ chlorine oxidation with a fluence of 1000 mJ/cm^2 in raw water, pre-DAFF, and post-BAC water samples except in pre-BAC water sample after 24 h. Chlorate concentrations were always below the guideline or recommended concentrations. According to Health Canada (2012), chlorate is regulated with a guideline set at 1 mg L^{-1} in drinking water. As chlorate is one of the leading products of chlorine photolysis it has to be carefully monitored. pH and chlorine dose may influence the formation of chlorate during chlorine photolysis, increasing the percentage of photolyzed free chlorine that can be converted to chlorate as shown in the above experiments.

5.4 AOX and Organic DBPs Formation

AOX is the sum of all halogeno organic substances and surrogate for the quantification of halogented DBPs. AOX concentration was higher in most samples after UV/chlorine treatment compared to dark chlorination. The AOX data obtained in this study indicate that the decomposition of NOM can form organic precursors which react with free chlorine rapidly to generate AOX species.

The four THMs, i.e., TCM, TBM, BDCM, and DBCM were formed during both UV/Chlorine oxidation (1000 and 2000 mJ/cm^2) and dark chlorination, and their concentrations increased over time. For the CMPP water, after 40 min, UV treatment had an impact and a decrease in TTHMs formation was observed over dark chlorination. After 24h the TTHMs were much higher but the same trend was observed (Figure 14). Moreover, applying a UV dose of 2000 mJ/cm^2 mitigated the TTHMs formation by 62.8% compared to a UV dose of 1000 mJ/cm^2. It is also interesting to notice that THMs and AOX (Figure 12) exhibit different behavior and therefore it can be con-

1332 cluded that THMs are not a good surrogate for the total formation of halogenated or-
1333 ganic compounds. For the MWTP water a different trend was observed, TTHMs for-
1334 mation was lower for UV/chlorine compared to dark chlorination for the raw water
1335 and a higher formation for the pre-DAFF, the pre-BAC and the post-BAC (Figure 15).
1336 This trend is opposite to the AOX formation during UV/chlorine treatment (Figure
1337 13). During UV/Chlorine oxidation, the increased in TTHMs concentration indicates
1338 that the reactive oxidants formed during chlorine photolysis are more efficient at gen-
1339 erating THMs than in dark chlorination for pre-DAFF, pre-BAC and post-BAC. Fur-
1340 thermore, RCS may be involved in the formation of THMs.

1341 Only DCAN and DBAN out of the 6 HANs analysed were detected in the CMPP
1342 water samples (Figure 16). The total formation of DCAN and BCAN increased after
1343 UV/Chlorine (1000 mJ/cm^2) treatment and 20 min contact time over dark chlorination.
1344 Moreover, the formation of DCAN was decreased by increasing the UV dose from
1345 1000 mJ/cm^2 to 2000 mJ/cm^2. Similarly, the total concentration of BCAN was im-
1346 pacted by UV treatment after 24h contact time, the THANs is deeply mitigated by the
1347 UV/Chlorine treatment with 137.5 µg/L and 288.9 µg/L compared to 884.0 µg/L for
1348 the dark chlorination. Figure 16 suggests that THANs formation was impacted by
1349 increasing UV dose and contact time which means that HANs precursors were decayed
1350 in chlorine photolysis. Moreover, these results indicate that radical reactions mediated
1351 THANs formation. DCAN, BCAN and CAN were formed at different a stage of the
1352 water treatment plant both during dark chlorination and UV/chlorine oxidation (Figure
1353 17). The application of UV decreased the THANs in the raw water and pre-BAC sam-
1354 ples but an increase was observed for the pre-DAFF and post-BAC samples over dark
1355 chlorination. The speciation was dominated by DBAN followed by BCAN and low
1356 concentrations of DCAN for all experiments.

1357 For HAA, only DCAA and BCAA were detected in the CMPP water samples after
1358 dark chlorination and UV/chlorine oxidation (1000 and 2000 mJ/cm^2) (Figure 18). The
1359 formation of DCAA and BCAA increased significantly during UV/chlorine oxidation
1360 compared to dark chlorination after 20 min and 24 h. Total HAAs formation increased
1361 significantly during UV/chlorine oxidation compared to dark chlorination. Radicals
1362 such as RCSs produced during chlorine photolysis might magnify HAA formation by
1363 interacting with HAA precursors. The total HAAs concentration after dark chlorina-
1364 tion and UV/chlorine oxidation (1000 mJ/cm^2) decreased along the treatment train

1365 (Figure 19) similar to the DOC concentration (Figure 7), respectively. MCAA, DCAA,
1366 BCAA, DBAA, and MBAA were formed in all MWTP water samples during dark
1367 chlorination and UV/chlorine oxidation (1000 mJ/cm^2) after 24 h. The speciation of
1368 the HAAs is different from the CMMP sample with a higher abundance of brominated
1369 HAAs. The THAAs concentration was decreased slightly during UV/chlorine oxida-
1370 tion (1000 mJ/cm^2) for raw water and post-BAC over dark chlorination while THAAs
1371 concentration was increased in pre-DAFF and pre-BAC samples after 24 h.

1372 Only DCP and TCP out of the four HKs analysed were detected in the CMPP water
1373 samples (Figure 20). The formation of DCP and TCP increased significantly during
1374 UV/chlorine oxidation over dark chlorination after 20 min, 40 min, and 24 h. The trend
1375 is different after 24 h with an increased concentration of THKs from dark chlorination
1376 to UV/chlorine at a dose of 1000 mJ/cm^2 and a decrease at a dose of 2000 mJ/cm^2. The
1377 abundance of THKs formed during UV/chlorine oxidation is higher than in dark chlo-
1378 rination. This might be due to the decomposition (for example, Cl-substitution and Cl-
1379 addition reactions) of HKs precursors by reactive chlorine species. Only TCP were
1380 formed at a different stage of the water treatment plant both during dark chlorination
1381 (except in post-BAC) and UV/chlorine oxidation while DCP was formed only in a raw
1382 water sample after dark chlorination (Figure 21). The formation of TCP is decreasing
1383 through the water treatment train after UV/chlorine oxidation. The application of UV
1384 decreased the HKs in the pre-DAFF and pre-BAC samples but an increase was ob-
1385 served for the raw water samples compared to dark chlorination. The speciation was
1386 dominated by TCP for all experiments.

1387 For HALs, only CH and DCAL were detected in the CMPP water samples (Figure 22)
1388 after dark chlorination and UV/chlorine oxidation (1000 and 2000 mJ/cm^2). The total
1389 HALs formation was increasing with increasing contact time with the oxidant. The
1390 concentration of CH and DCAL was higher during UV/chlorine oxidation compared
1391 to dark chlorination after 20 min, 40 min, and 24 h. The higher formation of THAls in
1392 UV/chlorine oxidation suggests that the reactive oxidant formed in chlorin photolysis
1393 might enhance the formation of THALs. This clearly showed that the impact of UV is
1394 detrimental to the mitigation of HALs with 48.7% and 8.7% more THALs after 1000
1395 and 2000 mJ/cm^2 of UV compared to dark chlorination. Only CH and DCAL were
1396 formed at a different stage of the water treatment plant (MWTP) both during dark
1397 chlorination (except in pre-BAC and post-BAC) and UV/chlorine oxidation (Figure

23). The application of UV decreased the CH in the raw water, pre-DAFF and pre-BAC samples but no change was observed for the post-BAC samples over dark chlorination. The data indicate that CH precursors are not affected by reactive oxidants formed in chlorine photolysis, which suggests that CRS production during chlorine photolysis may not be involved in the formation of CH.

5.5 Concluding remarks

In conclusion, no clear trend could be extrapolated from the experiments for AOX, THMs and HANs formation. Total HAAs, THKs, and THALs formation increased significantly during UV/chlorine oxidation compared to dark chlorination. This clearly showed that the impact of UV is detrimental to the mitigation of HAAs, HKs and HALs. Depending on the UV dose and the water characteristic the UV/chlorine treatment could be beneficial in mitigating DBPs. In this case, the applied chlorine concentration and UV doses should be carefully adjusted based on the goal that needs to be achieved, i.e. keeping the DBPs below the guideline values or reducing the formation of AOX for example. As stated, before, the aim of this study was to understand the extent of DBPs formation under different scenarios. However, as presented in the report it is really difficult to draw firm conclusions on the benefit of using UV/Chlorine over dark chlorination since the effectiveness of the process is highly dependent on the water matrix. No clear trend could be drawn and different class of DBPs exhibits opposite behaviour. UV/Chlorine might be tuned and used for a particular application where one class of DBPs is targeted specifically. It will be interesting to analyse the cyto- and geno-toxicity of the different samples and compared them to the formation of DBPs. Hence, further study is needed to fully understand this complex system.

Future study are needed to improve our understanding of the system. For example investigating the effect of LP and MP lamp on DBPs formation during UV/chlorine oxidation, the degradation of key trace chemical contaminants (micropollutants), studying additional DBPs with a relevant toxicity level, studying the effect of different pH levels on chlorine degradation and DBPs formation.

Chapter 6: References

Alegre, M. L., Geronés, M., Rosso, J. A., Bertolotti, S. G., Braun, A. M., Mártire, D. O., & Gonzalez, M. C. (2000). Kinetic study of the reactions of chlorine atoms and Cl2.- radical anions in aqueous solutions. 1. Reaction with benzene. *Journal of Physical Chemistry A, Volume 104, Issue 14, Pages 3117 - 3125*. doi:10.1021/jp9929768

Allard, S., Charrois, J. W. A., Joll, C. A., & Heitz, A. (2012). Simultaneous analysis of 10 trihalomethanes at nanogram per liter levels in water using solid-phase microextraction and gas chromatography mass-spectrometry. *Journal of Chromatography A, 1238*, 15-21. doi:10.1016/j.chroma.2012.03.020

Allard, S., Fouche, L., Dick, J., Heitz, A., & von Gunten, U. (2013). Oxidation of Manganese(II) during Chlorination: Role of Bromide. *Environ. Sci. Technol, 47*(15), 8716-8723. doi:10.1021/es401304r

Allard, S., Tan, J., Joll, C. A., & von Gunten, U. (2015). Mechanistic Study on the Formation of Cl-/Br-/I-Trihalomethanes during Chlorination/Chloramination Combined with a Theoretical Cytotoxicity Evaluation. *Environ. Sci. Technol, 49*(18), 11105-11114. doi:10.1021/acs.est.5b02624

Amy, G. L., Chadik, P. A., King, P. H., & Cooper, W. J. (1984). Chlorine utilization during trihalomethane formation in the presence of ammonia and bromide. *Environ. Sci. Technol, 18*(10), 781-786. doi:10.1021/es00128a011

AWWA. (1999). Water quality and treatment : a handbook of community water supplies / American Water Works Association, Raymond D. Letterman, technical editor (5th ed.. ed.). New York: New York : McGraw-Hill.

Ben, W., Sun, P., & Huang, C.-H. (2016). Effects of combined UV and chlorine treatment on chloroform formation from triclosan. *Chemosphere, 150*, 715-722. doi:10.1016/j.chemosphere.2015.12.071

Bond, T., Goslan, E. H., Parsons, S. A., & Jefferson, B. (2012). A critical review of trihalomethane and haloacetic acid formation from natural organic matter surrogates. *Environmental technology reviews, 1*(1), 93-113. doi:10.1080/09593330.2012.705895

Bond, T., Templeton, M. R., & Graham, N. (2012). Precursors of nitrogenous disinfection by-products in drinking water—A critical review and analysis. *J Hazard Mater, 235-236*, 1-16. doi:10.1016/j.jhazmat.2012.07.017

Bulman, D. M., & Remucal, C. K. (2020). Role of Reactive Halogen Species in Disinfection Byproduct Formation during Chlorine Photolysis. *Environ. Sci. Technol, 54*(15), 9629-9639. doi:10.1021/acs.est.0c02039

Buxton, G. V., & Subhani, M. S. (1972a). Radiation chemistry and photochemistry of oxychlorine ions. Part 1.—Radiolysis of aqueous solutions of hypochlorite and chlorite ions. *Journal of the Chemical Society, Faraday Transactions 1: Physical Chemistry in Condensed Phases, 68*, 947. doi:10.1039/f19726800947

Buxton, G. V., & Subhani, M. S. (1972b). Radiation chemistry and photochemistry of oxychlorine ions. Part 2.—Photodecomposition of aqueous solutions of hypochlorite ions. *Journal of the Chemical Society, Faraday Transactions 1: Physical Chemistry in Condensed Phases, 68*, 958. doi:10.1039/f19726800958

Buxton, G. V., & Subhani, M. S. (1972c). Radiation chemistry and photochemistry of oxychlorine ions. Part 3.—Photodecomposition of aqueous solutions of chlorite ions. *Journal of the Chemical Society, Faraday Transactions 1: Physical Chemistry in Condensed Phases, 68*, 970. doi:10.1039/f19726800970

Canada, H. (2012). *Guidelines for Canadian Drinking Water Quality—Summery Table. Water, Air and Climate Change Bureau.* : Healthy Environments and Consumer Safety Branch, Health Canada, Ottawa, Ontario, Canada.

Carter, R. A. A., Allard, S., Croué, J.-P., & Joll, C. A. (2019). Occurrence of disinfection by-products in swimming pools and the estimated resulting cytotoxicity. *Science of the Total Environment, 664*, 851-864. doi:10.1016/j.scitotenv.2019.01.428

Carter, R. A. A., Liew, D. S., West, N., Heitz, A., & Joll, C. A. (2019). Simultaneous analysis of haloacetonitriles, haloacetamides and halonitromethanes in chlorinated waters by gas chromatography-mass spectrometry. *Chemosphere, 220*, 314-323. doi:10.1016/j.chemosphere.2018.12.069

Chow, A. T., Leech, D. M., Boyer, T. H., & Singer, P. C. (2008). Impact of Simulated Solar Irradiation on Disinfection Byproduct Precursors. *Environ. Sci. Technol, 42*(15), 5586-5593. doi:10.1021/es800206h

Chu, W., Gao, N., Krasner, S. W., Templeton, M. R., & Yin, D. (2012). Formation of halogenated C-, N-DBPs from chlor(am)ination and UV irradiation of tyrosine in drinking water. *Environmental Pollution, 161*, 8-14. doi:10.1016/j.envpol.2011.09.037

Corin, N., Backlund, P., & Kulovaara, M. (1996). Degradation products formed during UV-irradiation of humic waters. *Chemosphere (Oxford), 33*(2), 245-255. doi:10.1016/0045-6535(96)00167-1

Deng, L., Huang, C.-H., & Wang, Y.-L. (2014). Effects of Combined UV and Chlorine Treatment on the Formation of Trichloronitromethane from Amine Precursors. *Environ. Sci. Technol, 48*(5), 2697-2705. doi:10.1021/es404116n

Dotson, A. D., Keen, V. S., Metz, D., & Linden, K. G. (2010). UV/H 2O 2 treatment of drinking water increases post-chlorination DBP formation. *Water research (Oxford), 44*(12), 3703-3713. doi:10.1016/j.watres.2010.04.006

EUC. (1998). European Union Council Directive 98/83/EC 3 November 1998 on the Quality of Water Intended for Human Consumption, Off. J. Eur. Communities: Legis. : 330/32, 5 of December, 1998.

Fanali, S. (2013). Liquid chromatography . Applications / [edited by] Salvatore Fanali, Paul R. Haddad, David Lloyd, Colin F. Poole, Peter Schoenmakers. Amsterdam: Amsterdam : Elsevier.

Fang, J., Fu, Y., & Shang, C. (2014). The Roles of Reactive Species in Micropollutant Degradation in the UV/Free Chlorine System. *Environ. Sci. Technol, 48*(3), 1859-1868. doi:10.1021/es4036094

Gallard, H., Pellizzari, F., Croué, J. P., & Legube, B. (2003). Rate constants of reactions of bromine with phenols in aqueous solution. *Water Research, 37*(12), 2883-2892. doi:10.1016/S0043-1354(03)00132-5

Gao, Z.-C., Lin, Y.-L., Xu, B., Xia, Y., Hu, C.-Y., Zhang, T.-Y., . . . Gao, N.-Y. (2019). Effect of UV wavelength on humic acid degradation and disinfection by-product formation during the UV/chlorine process. *Water Research, 154*, 199-209. doi:10.1016/j.watres.2019.02.004

Gary, A. B., Vicki, D., June, K. D., Robert, E. C., Sid, H., Fred, H., . . . Robert, C. S. (1999). Drinking Water Disinfection Byproducts: Review and Approach to Toxicity Evaluation. *Environmental Health Perspectives, 107*(Supplement 1), 207-217. doi:10.1289/ehp.99107s1207

Glezer, V., Harris, B., Tal, N., Iosefzon, B., & Lev, O. (1999). Hydrolysis of haloacetonitriles: LINEAR FREE ENERGY RELATIONSHIP, kinetics and products. *Water research (Oxford), 33*(8), 1938-1948. doi:10.1016/S0043-1354(98)00361-3

Gunten, U. v., & Hoigne, J. (1994). Bromate formation during ozonation of bromide-containing waters: interaction of ozone and hydroxyl radical reactions. *Environmental Science & Technology, 28*(7), 1234.

Guo, K., Wu, Z., Shang, C., Yao, B., Hou, S., Yang, X., . . . Fang, J. (2017). Radical Chemistry and Structural Relationships of PPCP Degradation by UV/Chlorine Treatment in Simulated Drinking Water. *Environ. Sci. Technol, 51*(18), 10431-10439. doi:10.1021/acs.est.7b02059

Guo, K., Wu, Z., Yan, S., Yao, B., Song, W., Hua, Z., . . . Fang, J. (2018). Comparison of the UV/chlorine and UV/H2O2 processes in the degradation of PPCPs in simulated drinking water and wastewater: Kinetics, radical mechanism and energy requirements. *Water research (Oxford), 147*, 184-194. doi:10.1016/j.watres.2018.08.048

Hansen, K. M. S., Willach, S., Antoniou, M. G., Mosbæk, H., Albrechtsen, H.-J., & Andersen, H. R. (2012). Effect of pH on the formation of disinfection byproducts in swimming pool water – Is less THM better? *Water Research, 46*(19), 6399-6409. doi:10.1016/j.watres.2012.09.008

Hansen, K. M. S., Zortea, R., Piketty, A., Vega, S. R., & Andersen, H. R. (2013). Photolytic removal of DBPs by medium pressure UV in swimming pool water. *Science of the Total Environment, 443*, 850-856. doi:10.1016/j.scitotenv.2012.11.064

Heeb, M. B., Criquet, J., Zimmermann-Steffens, S. G., & von Gunten, U. (2014). Oxidative treatment of bromide-containing waters: Formation of bromine and its reactions with inorganic and organic compounds — A critical review. *Water Research, 48*, 15-42. doi:10.1016/j.watres.2013.08.030

Heller-Grossman, L., Manka, J., Limoni-Relis, B., & Rebhun, M. (2001). THM, haloacetic acids and other organic DBPs formation in disinfection of bromide rich Sea of Galilee (Lake Kinneret) water. *Water science & technology. Water supply, 1*(2), 259-266. doi:10.2166/ws.2001.0046

Höfl;, C., Sigl;, G., Specht;, O., Wurdack;, I., & Wabner, D. (1997). Oxidative degradation of aox and cod by different advanced oxidation processes: A comparative study with two samples of a pharmaceutical wastewater. *Water Science and Technology, 35*(4). doi:10.1016/S0273-1223(97)00033-4

Hua, G., Reckhow, D. A., & Kim, J. (2006). Effect of Bromide and Iodide Ions on the Formation and Speciation of Disinfection Byproducts during Chlorination. *Environ. Sci. Technol, 40*(9), 3050-3056. doi:10.1021/es0519278

Hua, L.-C., Chao, S.-J., Huang, K., & Huang, C. (2020). Characteristics of low and high SUVA precursors: Relationships among molecular weight, fluorescence, and chemical composition with DBP formation. *The Science of the total environment, 727*, 138638. doi:10.1016/j.scitotenv.2020.138638

Hua, Z., Li, D., Wu, Z., Wang, D., Cui, Y., & Huang, X. (2021). DBP formation and toxicity alteration during UV/chlorine treatment of wastewater and the effects of ammonia and bromide. *Water Research, 188*, 116549-116549. doi:10.1016/j.watres.2020.116549

Huang, K., & Shah, A. D. (2018). Role of tertiary amines in enhancing trihalomethane and haloacetic acid formation during chlorination of aromatic compounds and a natural organic matter extract. *Environmental science water research & technology, 4*(5), 663-679. doi:10.1039/c7ew00439g

Hur, J. (2011). Microbial Changes in Selected Operational Descriptors of Dissolved Organic Matters From Various Sources in a Watershed. *Water, Air, & Soil Pollution, 215*(1), 465-476. doi:10.1007/s11270-010-0491-0

Jing Li, & Blatchley, E. R. (2007). Combined application of UV radiation and chlorine: implications with respect to DBP formation and destruction in recreational water applications. Paper presented at the Proceedings of the Water Environment Federation Annual Technical Exhibition and Conference 2007, Disinfection BY-Products, San Diego, California, USA, 128–133.

Jo, C. H. (2008). Oxidation of Disinfection Byproducts and Algae-related Odorants by UV/Hydrogen Peroxide. In: ProQuest Dissertations Publishing.

Johannes, J. R. (1976). Haloforms in Drinking Water. *Journal - American Water Works Association, 68*(3), 168-172. doi:10.1002/j.1551-8833.1976.tb02376.x

Kang, N., Anderson, T. A., & Andrew Jackson, W. (2006). Photochemical formation of perchlorate from aqueous oxychlorine anions. *Anal Chim Acta, 567*(1), 48-56. doi:10.1016/j.aca.2006.01.085

Kristiana, I., Gallard, H., Joll, C., & Croué, J.-P. (2009). The formation of halogen-specific TOX from chlorination and chloramination of natural organic matter isolates. *Water Research, 43*(17), 4177-4186. doi:10.1016/j.watres.2009.06.044

Kristiana, I., McDonald, S., Tan, J., Joll, C., & Heitz, A. (2015). Analysis of halogen-specific TOX revisited: Method improvement and application. *Talanta, 139*, 104-110. doi:10.1016/j.talanta.2015.02.029

Kulovaara, M., Corin, N., Backlund, P., & Tervo, J. (1996). Impact of UV254-radiation on aquatic humic substances. *Chemosphere (Oxford), 33*(5), 783-790. doi:10.1016/0045-6535(96)00233-0

Kumar, K., & Margerum, D. W. (1987). Kinetics and mechanism of general-acid-assisted oxidation of bromide by hypochlorite and hypochlorous acid. *Inorg. Chem, 26*(16), 2706-2711. doi:10.1021/ic00263a030

Kuo, J., Chen, C.-l., & Nellor, M. (2005). Closure to "Standardized Collimated Beam Testing Protocol for Water/Wastewater Ultraviolet Disinfection" by Jeff Kuo, Ching-lin Chen, and Margaret Nellor. *Journal of Environmental Engineering, 129*(5), 828-829. doi:10.1061/(ASCE)0733-9372(2005)131:5(828)

Lado Ribeiro, A. R., Moreira, N. F. F., Li Puma, G., & Silva, A. M. T. (2019). Impact of water matrix on the removal of micropollutants by advanced oxidation technologies. *Chemical engineering journal (Lausanne, Switzerland : 1996), 363*, 155-173. doi:10.1016/j.cej.2019.01.080

Lee, M.-H., & Hur, J. (2014). Photodegradation-Induced Changes in the Characteristics of Dissolved Organic Matter with Different Sources and Their Effects on Disinfection By-Product Formation Potential. *Clean : soil, air, water, 42*(5), 552-560. doi:10.1002/clen.201200685

Lee, W., Lee, Y., Allard, S., Ra, J., Han, S., & Lee, Y. (2020). Mechanistic and Kinetic Understanding of the UV254 Photolysis of Chlorine and Bromine Species in Water and Formation of Oxyhalides. *Environ. Sci. Technol, 54*(18), 11546-11555. doi:10.1021/acs.est.0c02698

Lee, Y., & Gunten, U. v. (2009). Transformation of 17α-Ethinylestradiol during Water Chlorination: Effects of Bromide on Kinetics, Products, and Transformation Pathways. *Environ. Sci. Technol, 43*(2), 480-487. doi:10.1021/es8023989

Li, W., Jain, T., Ishida, K., Remucal, C. K., & Liu, H. (2017). Correction: A mechanistic understanding of the degradation of trace organic contaminants by UV/hydrogen peroxide, UV/persulfate and UV/free chlorine for water reuse. *Environmental science water research & technology, 3*(2), 377-377. doi:10.1039/c7ew90005h

Liu, W., Andrews, S. A., Bolton, J. R., Linden, K. G., Sharpless, C., & Stefan, M. (2002). Comparison of disinfection byproduct (DBP) formation from different UV technologies at bench scale. *Water science & technology. Water supply, 2*(5-6), 515-521. doi:10.2166/ws.2002.0212

Liu, W., Cheung, L.-M., Yang, X., & Shang, C. (2006). THM, HAA and CNCl formation from UV irradiation and chlor(am)ination of selected organic waters. *Water Research, 40*(10), 2033-2043. doi:10.1016/j.watres.2006.03.019

Liu, W., Zhang, Z., Yang, X., Xu, Y., & Liang, Y. (2012). Effects of UV irradiation and UV/chlorine co-exposure on natural organic matter in water. *Science of the Total Environment, 414*, 576-584. doi:10.1016/j.scitotenv.2011.11.031

Lyon, B. A., Dotson, A. D., Linden, K. G., & Weinberg, H. S. (2012). The effect of inorganic precursors on disinfection byproduct formation during UV-chlorine/chloramine drinking water treatment. *Water Research, 46*(15), 4653-4664. doi:10.1016/j.watres.2012.06.011

Malley Jr., J. P., Shaw, J. P., & Ropp, J. R. (1995). Evaluation of by-products produced by treatment of groundwaters with ultraviolet irradiation. *American Water Works Association Research Foundation*.

Marion, B., Weinberg, H., Dotson, A., & Linden, K. (2010). Impact of UV-chlorine/chloramine drinking water treatment on DBP formation in bromide- and nitrate-containing waters. *Water Quality Technology Conference and Exposition 2010*, 2740-2746.

Markus Langsa Sebastien Allard Ina Kristiana Anna Heitz Cynthia, A. J. (2017). Halogen-specific total organic halogen analysis : Assessment by recovery of total

bromine. *Journal of Environmental Sciences, 58*(8), 340-348. doi:10.1016/j.jes.2017.06.010

Matilainen, A., & Sillanpää, M. (2010). Removal of natural organic matter from drinking water by advanced oxidation processes. *Chemosphere, 80*(4), 351-365. doi:10.1016/j.chemosphere.2010.04.067

Mercier Shanks, C., Sérodes, J.-B., & Rodriguez, M. J. (2013). Spatio-temporal variability of non-regulated disinfection by-products within a drinking water distribution network. *Water Research, 47*(9), 3231-3243. doi:10.1016/j.watres.2013.03.033

Muellner, M. G., Wagner, E. D., McCalla, K., Richardson, S. D., Woo, Y.-T., & Plewa, M. J. (2007). Haloacetonitriles vs. Regulated Haloacetic Acids: Are Nitrogen-Containing DBPs More Toxic? *Environ. Sci. Technol, 41*(2), 645-651. doi:10.1021/es0617441

Neale, P., Antony, A., Bartkow, M., Farre, M., Heitz, A., & Kristiana, I. (2012). Bioanalytical assessment of the formation of disinfection byproducts in a drinking water treatment plant.

Neale, P. A., Antony, A., Bartkow, M. E., Farré, M. J., Heitz, A., & Kristiana, I. (2012). Bioanalytical Assessment of the Formation of Disinfection Byproducts in a Drinking Water Treatment Plant. *Environ. Sci. Technol, 46*(18), 10317-10325. doi:10.1021/es302126t

Nieuwenhuijsen, M. J., Toledano, M. B., Eaton, N. E., Fawell, J., & Elliott, P. (2000). Chlorination disinfection byproducts in water and their association with adverse reproductive outcomes: a review. *Occup Environ Med, 57*(2), 73-85. doi:10.1136/oem.57.2.73

Nihemaiti, M., Miklos, D. B., Hübner, U., Linden, K. G., Drewes, J. E., & Croué, J.-P. (2018). *Removal of trace organic chemicals in wastewater effluent by UV/H2O2 and UV/PDS* (Vol. 145). England: England: Elsevier BV.

Nowell, L. H., & Hoigné, J. (1992). Photolysis of aqueous chlorine at sunlight and ultraviolet wavelengths—II. Hydroxyl radical production. *Water Research, 26*(5), 599-605. doi:10.1016/0043-1354(92)90233-T

NWQMS. (2011). *Australian Drinking Water Guidlines 6, Version 3.4 Updated October 2017* Canberra ACT: National Water Quality Management Strategy. National Health and Medical Research Council.

Pisarenko, A. N., Stanford, B. D., Snyder, S. A., Rivera, S. B., & Boal, A. K. (2013). Investigation of the use of Chlorine Based Advanced Oxidation in Surface Water: Oxidation of Natural Organic Matter and Formation of Disinfection Byproducts. *Journal of Advanced Oxidation Technologies, 16 (1)*, 137-150. doi:10.1515/jaots-2013-0115

Plewa, M. J., Muellner, M. G., Richardson, S. D., Fasano, F., Buettner, K. M., & Woo, Y.-T. (2008). Occurrence, Synthesis, and Mammalian Cell Cytotoxicity and Genotoxicity of Haloacetamides: An Emerging Class of Nitrogenous Drinking Water Disinfection Byproducts. *Environ. Sci. Technol, 42*(3), 955-961. doi:10.1021/es071754h

Plewa, M. J., Simmons, J. E., Richardson, S. D., & Wagner, E. D. (2010). Mammalian cell cytotoxicity and genotoxicity of the haloacetic acids, a major class of drinking water disinfection by-products. *Environmental and Molecular Mutagenesis, 51*(8-9), 871-878. doi:10.1002/em.20585

Plewa, M. J., Wagner, E. D., Jazwierska, P., Richardson, S. D., Chen, P. H., & McKague, A. B. (2004). Halonitromethane Drinking Water Disinfection Byproducts: Chemical Characterization and Mammalian Cell Cytotoxicity and Genotoxicity. *Environmental Science and Technology, 38*(1), 62-68. doi:10.1021/es030477l

Plewa, M. J., Wagner, E. D., Metz, D. H., Kashinkunti, R., Jamriska, K. J., & Meyer, M. (2012). Differential toxicity of drinking water disinfected with combinations of ultraviolet radiation and chlorine. *Environmental Science and Technology, 46*(14), 7811-7817. doi:10.1021/es300859t

Plewa, M. J., Wagner, E. D., Metz, D. H., Kashinkunti, R., Jamriska, K. J., & Meyer, M. (2012). Differential Toxicity of Drinking Water Disinfected with Combinations of Ultraviolet Radiation and Chlorine. *Environ. Sci. Technol, 46*(14), 7811-7817. doi:10.1021/es300859t

Plewa, M. J., Wagner, E. D., Muellner, M. G., Hsu, K.-M., & Richardson, S. D. (2008a). Comparative Mammalian Cell Toxicity of N-DBPs and C-DBPs. In T. Karanfil, S. W. Krasner, & Y. Xie (Eds.), *Disinfection by-Products in Drinking Water: Occurrence, Formation, Health Effects, and Control* (Vol. 995, pp. 36-50).

Plewa, M. J., Wagner, E. D., Muellner, M. G., Hsu, K.-M., & Richardson, S. D. (2008b). Comparative Mammalian Cell Toxicity of N-DBPs and C-DBPs. In. Washington, DC: Washington, DC: American Chemical Society.

Plewa, M. J., Wagner, E. D., Muellner, M. G., Hsu, K.-M., & Richardson, S. D. (2008c). Comparative Mammalian Cell Toxicity of N-DBPs and C-DBPs. In *Disinfection By-Products in Drinking Water* (Vol. 995, pp. 36-50): American Chemical Society.

Ramesh D, K., Karl G, L., Gwy-Am, S., Deborah H, M., Mark D, S., Melissa C, M., & Amy M, S. (2004). Investigating Multibarrier inactivation for Cincinnati—UV, BY-PRODUCTS, AND BIOSTABILITY. *Journal - American Water Works Association, 96*(6), 114-127. doi:10.1002/j.1551-8833.2004.tb10785.x

Reckhow, D. A., Linden, K. G., Kim, J., Shemer, H., & Makdissy, G. (2010). Effect of UV treatment on DBP formation. *Journal - American Water Works Association, 102*(6), 100-113. doi:10.1002/j.1551-8833.2010.tb10134.x

Remucal, C. K., & Manley, D. (2016). Emerging investigators series: the efficacy of chlorine photolysis as an advanced oxidation process for drinking water treatment. *Environmental science water research & technology, 2*(4), 565-579. doi:10.1039/C6EW00029K

Richardson, S. (2003). Disinfection by-products and other emerging contaminants in drinking water. *TrAC, Trends in analytical chemistry (Regular ed.), 22*(10), 666-684. doi:10.1016/s0165-9936(03)01003-3

Richardson, S., Plewa, M., Wagner, E., Schoeny, R., & Demarini, D. (2007). Occurrence, genotoxicity, and carcinogenicity of regulated and emerging disinfection

by-products in drinking water: A review and roadmap for research. *Mutation research. Reviews in mutation research, 636*(1-3), 178-242. doi:10.1016/j.mrrev.2007.09.001

Salhi, E., & von Gunten, U. (1999). Simultaneous determination of bromide, bromate and nitrite in low µg/L levels by ion chromatography without sample pre-treatment.

Serrano, M., Silva, M., & Gallego, M. (2014). Fast and "green" method for the analytical monitoring of haloketones in treated water. *Journal of Chromatography A, 1358*, 232-239. doi:10.1016/j.chroma.2014.06.103

Serrano, M., Silva, M., & Gallego, M. (2015). Determination of 14 haloketones in treated water using solid–phase microextraction and gas chromatography–mass spectrometry. *Journal of Chromatography A, 1407*, 208-215. doi:10.1016/j.chroma.2015.06.060

Shah, A. D., Dotson, A. D., Linden, K. G., & Mitch, W. A. (2011). Impact of UV Disinfection Combined with Chlorination/Chloramination on the Formation of Halonitromethanes and Haloacetonitriles in Drinking Water. *Environ. Sci. Technol, 45*(8), 3657-3664. doi:10.1021/es104240v

Sichel, C., Garcia, C., & Andre, K. (2011). Feasibility studies: UV/chlorine advanced oxidation treatment for the removal of emerging contaminants. *Water Research, 45*(19), 6371-6380. doi:10.1016/j.watres.2011.09.025

Smith, E. M., Plewa, M. J., Lindell, C. L., Richardson, S. D., & Mitch, W. A. (2010). Comparison of byproduct formation in waters treated with chlorine and iodine: Relevance to point-of-use treatment. *Environmental Science and Technology, 44*(22), 8446-8452.

Sun, P., Lee, W.-N., Zhang, R., & Huang, C.-H. (2016). Degradation of DEET and Caffeine under UV/Chlorine and Simulated Sunlight/Chlorine Conditions. *Environ. Sci. Technol, 50*(24), 13265-13273. doi:10.1021/acs.est.6b02287

Tchobanoglous, G., Burton, F. L., Stensel, H. D., Metcalf, & Eddy. (2003). *Wastewater engineering : treatment and reuse / Metcalf & Eddy, Inc* (4th ed. / revised by George Tchobanoglous, Franklin L. Burton, H. David Stensel.. ed.). Boston: Boston : McGraw-Hill.

Toor, R., & Mohseni, M. (2007). UV-H2O2 based AOP and its integration with biological activated carbon treatment for DBP reduction in drinking water. *Chemosphere, 66*(11), 2087-2095. doi:10.1016/j.chemosphere.2006.09.043

USEPA. (1999). *Alternative Disinfectants and Oxidants Guidance Manual*: United States Environmental Protection Agency.

USEPA. (2002). The occurrence of disinfection by-products (DBPs) of health concern in drinking water: results of a nationwide DBP occurrence study: United States Environmental Protection Agency.

USEPA. (2006). *Drinking Water Standards and Health Advisories*: United States Environmental Protection Agency. Washington, DC.

Wang, C., Moore, N., Bircher, K., Andrews, S., & Hofmann, R. (2019). Full-scale comparison of UV/H2O2 and UV/Cl2 advanced oxidation: The degradation of micropollutant surrogates and the formation of disinfection byproducts. *Water research (Oxford), 161*, 448-458. doi:10.1016/j.watres.2019.06.033

Wang, D., Bolton, J. R., Andrews, S. A., & Hofmann, R. (2015). Formation of disinfection by-products in the ultraviolet/chlorine advanced oxidation process. *Science of the Total Environment, 518-519*, 49-57. doi:10.1016/j.scitotenv.2015.02.094

Wang, J., & Wang, S. (2020). Reactive species in advanced oxidation processes: Formation, identification and reaction mechanism. *Chemical engineering journal (Lausanne, Switzerland : 1996), 401*, 126158. doi:10.1016/j.cej.2020.126158

Wang, W.-L., Zhang, X., Wu, Q.-Y., Du, Y., & Hu, H.-Y. (2017). Degradation of natural organic matter by UV/chlorine oxidation: Molecular decomposition, formation of oxidation byproducts and cytotoxicity. *Water Research, 124*, 251-258. doi:10.1016/j.watres.2017.07.029

Watts, M. J., & Linden, K. G. (2007). Chlorine photolysis and subsequent OH radical production during UV treatment of chlorinated water. *Water Research, 41*(13), 2871-2878. doi:10.1016/j.watres.2007.03.032

Weishaar, J. L., Aiken, G. R., Bergamaschi, B. A., Fram, M. S., Fujii, R., & Mopper, K. (2003). Evaluation of Specific Ultraviolet Absorbance as an Indicator of the Chemical Composition and Reactivity of Dissolved Organic Carbon. *Environ. Sci. Technol, 37*(20), 4702-4708. doi:10.1021/es030360x

Weng, S., Li, J., & Blatchley, E. R. (2012). Effects of UV254 irradiation on residual chlorine and DBPs in chlorination of model organic-N precursors in swimming pools. *Water research (Oxford), 46*(8), 2674-2682. doi:10.1016/j.watres.2012.02.017

Westerhoff, P., Chao, P., & Mash, H. (2004). Reactivity of natural organic matter with aqueous chlorine and bromine. *Water Research, 38*(6), 1502-1513. doi:10.1016/j.watres.2003.12.014

WHO. (1993). *Guidelines for Drinking-water Quality, second ed.*: World Health Organization. Geneva.

WHO. (2011). *Guidelines for Drinking-water Quality*: World Health Organization. Geneva.

Xiang, Y., Fang, J., & Shang, C. (2016). Kinetics and pathways of ibuprofen degradation by the UV/chlorine advanced oxidation process. *Water Research, 90*, 301-308. doi:10.1016/j.watres.2015.11.069

Yang, X., Shang, C., & Westerhoff, P. (2007). Factors affecting formation of haloacetonitriles, haloketones, chloropicrin and cyanogen halides during chloramination. *Water Research, 41*(6), 1193-1200. doi:10.1016/j.watres.2006.12.004

Yang, Y., Komaki, Y., Kimura, S. Y., Hu, H. Y., Wagner, E. D., Mariñas, B. J., & Plewa, M. J. (2014). Toxic impact of bromide and iodide on drinking water disinfected with chlorine or chloramines. *Environmental Science and Technology, 48*(20), 12362-12369. doi:10.1021/es503621e

Yang, Y., Pignatello, J. J., Ma, J., & Mitch, W. A. (2016). Effect of matrix components on UV/H2O2 and UV/S2O82− advanced oxidation processes for trace organic degradation in reverse osmosis brines from municipal wastewater reuse facilities. *Water research (Oxford), 89*, 192-200. doi:10.1016/j.watres.2015.11.049

Yeom, Y., Han, J., Zhang, X., Shang, C., Zhang, T., Li, X., . . . Dionysiou, D. D. (2021). A review on the degradation efficiency, DBP formation, and toxicity variation in the UV/chlorine treatment of micropollutants. *Chemical engineering journal (Lausanne, Switzerland : 1996), 424*, 130053. doi:10.1016/j.cej.2021.130053

Zhang, X., Li, W., Blatchley, E. R., Wang, X., & Ren, P. (2015). UV/chlorine process for ammonia removal and disinfection by-product reduction: Comparison with chlorination. *Water Research, 68*, 804-811. doi:10.1016/j.watres.2014.10.044